EVALUATION OF DAMPING COEFFICIENTS OF A VIBRATORY MODEL OF HUMAN BODY

A Thesis

Submitted In partial fulfillment of the requirement for the award of degree of

MASTER OF ENGINEERING

IN

CAD/CAM & ROBOTICS

Submitted By

Mayank Mishra

80681013

Under the guidance of

Dr. S. P. Nigam

Visiting Professor, MED

TU, Patiala-147004

Mechanical Engineering Department

Thapar University

Patiala-147004 (INDIA)

June, 2008

Certificate

I hereby certify that the work which is being presented in the thesis entitled, ***"Evaluation Of Damping Coefficients Of a Vibratory Model Of Human Body"****, in partial fulfillment of the requirements for the award of degree of* ***Master of Engineering in Mechanical Engineering*** *with specialization in* ***CAD/CAM & ROBOTICS*** *at* ***Thapar University****, Patiala, is an authentic record of my own work carried out under the supervision of* ***Dr.S.P.Nigam*** *and refers other researcher's works which are duly listed in the reference section.*

The matter embodied in this thesis has not been submitted for the award of any other degree of this or any other university.

Mayank Mishra,

(MAYANK MISHRA)

This is to certify that the above statement made by the candidate is correct and true to the best of my knowledge.

24/06/08

Dr. S. P. NIGAM
Visiting Professor
Mechanical Engineering Department.
Thapar University,
Patiala

9/7/2008

Dr. S.K. MOHAPATRA
Professor and Head,
Mechanical Engineering Department,
Thapar University,
Patiala-147004.

Dr. R.K. SHARMA
Dean of Academic Affairs,
Thapar University
Patiala -147004

ACKNOWLEDGEMENT

A thesis cannot be completed without the help of many people who contribute directly or indirectly through their constructive criticism in the evolution and preparation of this work. A special debt of gratitude is owed to my thesis supervisor, Dr. S.P. Nigam (Visiting professor M.E.D) for his gracious efforts and keen pursuit which has remained as a valuable asset for the successful fulfillment of my thesis. His dynamism and diligent enthusiasm have been highly instrumental in keeping my spirits high. His flawless & forthright suggestions blended with an innate intelligent application have crowned my task with success.

I would also like to offer my sincere thanks to all faculty, teaching and non-teaching, of Mechanical Engg. Deptt. (MED), and staff of central library, TU, Patiala for their assistance.

I am also thankful to the authors whose works I have consulted and quoted in this work. Last, but not the least, very special thanks to my parents and my friends for their constant encouragement and best wishes. Their patience and understanding without which this study would not have been in this present form, is greatly appreciated.

DATE **MAYANK MISHRA**

(80681013)

ABSTRACT

In this work, modeling of vibratory system of human body and its study under standing posture have been presented. The human body is developed as a spring-mass-damper system. A generalized procedure for modeling of human body through anthropomorphic model has been developed and assumptions are clearly stated. The model parameters are obtained through the mass, stiffness and damping values of the segment of the anthropomorphic model. The mass and stiffness values of the segments are obtained using the anthropometric data and elastic moduli of bones and tissues. An initial effort was made to consider the viscosity of blood and other fluids in predicting the behavior of the multi-degree damped vibratory systems. Damping is incorporated by assigning some appropriate clearance values to the individual segments. The damping coefficients and damping ratio values of individual segments are obtained using anthropometric data and viscosity of blood. The validation of modeling procedure is done by first developing the model for a 50^{th} percentile US male and comparing the response with some experimental response data of US male available in the literature. In addition this work also presents the frequency response of different parts of the body due to constant force excitation at foot and at hands.

The thesis seems to have achieved its objective with a fair success. On the basis of this work, vibratory models of individuals can be framed which can predict the actual frequency response with reasonable accuracy.

CONTENTS

LIST OF FIGURES

LIST OF TABLES

NOMENCLATURE

Symbol	Description
a_i, b_i, c_i	Semi-axes of an ellipsoid x,y and z axes
C_i	Damping constant of i^{th} damper element in the model
d_i	Half length of truncated ellipsoid
D_m	Mean diameter of piston and cylinder
D_i	Diameter of the ellipsoidal segment
E	Elastic modulus of ellipsoid segment
E_b	Elastic modulus of bone
E_t	Elastic modulus of tissue
F	Excitation force
I	Moment of Inertia
K_i	Stiffness of the spring element in the model
l	Length of the piston
L	Length of the segment
M_i	Mass of i^{th} ellipsoidal segment and mass element in the vibratory model
S_i	Axial stiffness of the ellipsoidal segment
t_r	Truncation Factor
X	Generalized displacement of the vibratory model
$\dot{X}$	Generalized velocity of the vibratory model
$\ddot{X}$	Generalized acceleration of the vibratory model

β_i	Damping coefficient of the i^{th} segment
ξ_i	Damping ratio of i^{th} ellipsoidal segment
δl	Deflection of spring
ω	Excitation frequency
μ	Effective coefficient of viscosity of blood and other fluid
[M]	Mass matrix of the vibratory model
[K]	Stiffness matrix of the vibratory model
[C]	Damping matrix of the vibratory model

Chapter-1

INTRODUCTION

Human body vibration is a phenomenon affecting millions of workers in the world. Among these are light and heavy equipment operators, m/c tool operators and truck drivers. Many harmful side effects of the vibration can be both physiological and neurological which in many cases lead to permanent injury. High speed vehicles frequently transmit dynamic forces to their occupants. Depending upon the intensity and duration of such disturbances, serious impairment of operator or passenger functioning may occur. These problems have led to extensive research directed towards defining and understanding the dynamics of the human body. Other endeavors such as health and medical studies and even athletic interests have also created a desire for comprehensive human dynamic analysis.

One approach to understand the human body vibration is through mathematical model. Mathematical modeling is an acceptable tool in engineering and many areas of the physical sciences. If the model can be shown to be reliable, it is an effective, economical and versatile method of studying the response of a system due to a wide variety of input conditions. The human body obviously consists of multitudes of interconnected masses, springs and dampers and should therefore behave as a dynamic system with many degree of freedom. One approach to understand the human body vibration is via a suitably formulated mathematical model that duplicates measured human body frequency response.

A properly matched model would indicate the source of measured human body characteristics, such as resonance peaks, that would be difficult to determine directly from a subject. There are many mathematical models proposed to duplicate human body vibration response, several of these models are inadequate in more ways than one. For example either they do not resemble human anatomy, or they do not match measured human frequency response, or they do not provide values for their lumped parameters. One of the major difficulties in modeling and evaluating human body response to vibration arises from the nature of the human body itself. There is no “Standard” human body due to variation in size, age, sex and weight etc. Another complexity in testing human subjects is that a human subject may not necessarily be passive and inanimate. A subject during vibratory testing can

easily change his posture and muscle and may even initiate motion on his own to offset personal undesirable movements. Such characteristics as breathing, swallowing, and fidgeting can add further difficulty.

The identification of mathematical model for a structural system entails the identification of mass, stiffness and damping matrices that consistently predict the dynamic responses of the structure as well as the loads on the structure, which are responsible for responses measured under operating conditions. While there are a variety of rational techniques for identifying the mass and stiffness matrices, eg, the lumped parameter, and the finite elements techniques, the method for obtaining the damping matrix has not achieved a comparable level of confidence in human body vibration. The difficulty is because the damping mechanism in real structure is not quite readily modeled from a simple physical description of the structure. In fact realistic estimates occurring in a vibrating structure are obtainable only from an experimental measurement. This work takes a small step forward by considering human body as a combination of spring and dampers. This thesis presents the formulation of human body model as a damped system.

Chapter-2

HUMAN BODY VIBRATION

2.1 Introduction

Human body vibration is a phenomenon affecting millions of worker in the world. Among these are light and heavy equipments operators, m/c tool operator and truck driver. Many harmful side effects of the vibration can be both physiological and neurological which in many cases lead to permanent injury. High speed vehicles frequently transmit dynamic forces to their occupants. Depending upon the intensity and duration of such disturbances, serious impairment of operator or passenger functioning may occur. These problems have led to extensive research directed towards defining and understanding the dynamic response of the human body. Recently there has been increased interest in the dynamics of the human body. Other endeavors such as health and medical studies and even athletic interests have also created a desire for comprehensive human dynamics analysis.

It is common to distinguish two different types of vibration exposure [17]:

Whole-body vibration: occurring when the body is supported on a vibrating surface, usually a seat or floor; and

Hand-transmitted vibration: involving contact with the source of motion at the fingers or in the hand.

2.1.1 Effects of whole-body vibration

Human exposure to vibration can produce various sensations (including pleasure, discomfort and pain) and interfere with a wide range of activities (such as reading and hand control movements).

Vibration of the body can also cause physiological and pathological effects. Low frequency oscillations of the body (with a frequency below about 0.5 Hz) can cause motion sickness.

The three criteria often used to judge the severity of exposures to whole-body vibration are: reduced comfort, interference with activities, and impaired health. These are vague concepts which require more precise definition before they can be used to define a vibration limit.

For example, a vibration limit for the preservation of health should indicate:

(i) The disorder caused by vibration;

(ii) The severity of the disorder corresponding to the limit;

(iii) The prevalence of the condition corresponding to the limit; and

(iv) A method of measuring vibration with respect to the limit.

Comfort: - Studies have yielded sufficient information on subjective responses for the reliable comparison of the discomfort produced by most common vibration exposures--this information is used by vehicle designers.

Performance: - The effects of vibration on activities are highly dependent on the activity. A vibration limit for the preservation of performance is therefore meaningless without a description of the task. Very often, any effect of vibration can be reduced by designing the task to be less susceptible to vibration effects.

Health: - Knowledge of the effects of vibration on health is far from complete. The most consistent reports concern disorders of the back-especially among drivers of off-road vehicles. However, all back problems in vibration environments cannot be automatically attributed to vibration exposure. There is currently no known disorder which is uniquely caused by vibration.

Many other causes of back disorders are well known (e.g., poor sitting postures, lifting excessive loads, lifting with a poor posture). Those conducting epidemiological studies also have difficulty in defining the severity of vibration exposures received by workers--the vibration is often complex and varies with time and the true severity of vibration depends on variables in addition to the measured vibration (e.g., sitting posture).

Some reported effects of whole-body vibration are difficult to distinguish from, for example, the effects of poor sitting postures, heavy lifting and aging. The most frequently reported groups of disorders are those which might be attributed to degenerative changes of the spine.

Vibration is not, however, the only cause of low back morbidity. Large variations in individual susceptibility to degenerative changes, the high incidence of degeneration in the general public and the varied selection procedures for occupations can often obscure an effect of a particular environmental stress.

The symptoms of low back pain often appear before degenerative changes are radiologically detectable-though prolonged periods of such symptoms often result in the eventual diagnosis of disc degeneration.

One of the proposed mechanisms of the action of vibration is the induction of micro fractures at the endplates with a callus formed during healing (or some other change to the endplate) reducing nutrient diffusion. Displacement of intervertebral discs has been reported as being associated with the vibration in off-road vehicles, trucks and cars.

However, studies have not normally been able to control all possible causes of such signs and symptoms and many have relied on individuals' reports of adverse effects. Some discretion is required before attributing such symptoms in an individual case to an occupational vibration exposure.

2.1.2 Causes of disorders

The environments which may be expected to be associated with whole-body vibration injuries are those in which vibration can be recognized as a source of discomfort: off-road vehicles (e.g., tractors, forest machines and earth-moving machinery), road vehicles (e.g., trucks, buses and cars), helicopters, high speed marine craft, industrial machinery and similar environments.

2.1.3 Variables

The four principal variables involved in the measurement of vibration exposures are [17]:

(i) Vibration magnitude;

(ii) Vibration frequency;

(iii) Vibration direction (or axis); and

(iv) Vibration duration

A major influence on all responses to vibration is body posture. The transmissions of vibration to the body, and the effects of vibration on the body, are highly dependent on body posture. The effects of whole-body vibration therefore vary greatly between individuals and between environments according to the body postures.

Postures may make the difference between acceptable and unacceptable conditions. What is considered comfortable in one vehicle may not be considered comfortable in another.

The vibration may interfere with hand control or vision with one set of displays and controls but not with another set of displays and controls.

2.2 MEASUREMENTS AND ANALYSIS OF VIBRATION EXPOSURES

The measurement and analysis of vibration involves converting an oscillatory movement necessarily lead to values which directly indicate the severity of the vibration exposures--but it is desirable that they are compatible with the evaluation procedure which does indicate vibration severity. Often, convenient engineering methods are used for measurement and the evaluation method is adapted to accommodate this convenience [17].

2.2.1 Vibration measurement

- Vibration is measured at the principal interfaces between the body and the vibrating environment. Figure 1.shows some of the axes which may need to be considered. Often, only a few of those illustrated need be included--although the axes to be included will depend on the environment.

- In some environments an adequate consideration of the vibration requires the inclusion of additional axes (e.g., vibration of the hands). The vibration is usually measured at the seat interfaces using accelerometers housed in mounts designed so that they do not abnormally compress the seat or distort the posture of the human body.

- Measurements on seats must always be made with a person seated on the seat since the body impedance will affect the transmission of vibration through the seat. Measurements made on the floor beneath a seat will not give a reliable indication of the vibration exposure of a seated person unless the seat is rigid and there is no rotational motion.

- Signals from accelerometers will often be recorded by analogue or digital means for subsequent analysis. A vibration meter can easily be constructed to give a short-term average indication of vibration magnitude if this is required.

- However, the time-varying characteristics of vibration exposures, the frequency-dependence of both human response and vehicle dynamics make it attractive to conduct some form of frequency analysis. This analysis may indicate a way of reducing vibration exposure by using a seat with a different dynamic response.

2.2.2 Vibration analysis

The analysis of vibration is frequently undertaken to determine the frequency content of the vibration. It may also be used to show how the vibration varies with time. Vibration analysis will aid an understanding of the causes of any high values and is often a necessary step towards alleviating any problem.

The average frequency content determined over a finite period of vibration exposure is shown by a spectra. Third-octave band spectra have often been used-octave band spectra are too coarse since both human responses and the dynamic responses of structures can vary rapidly with frequency. Modern spectral analysis is conducted using digital techniques and often results in the determination of constant bandwidth power spectral densities.

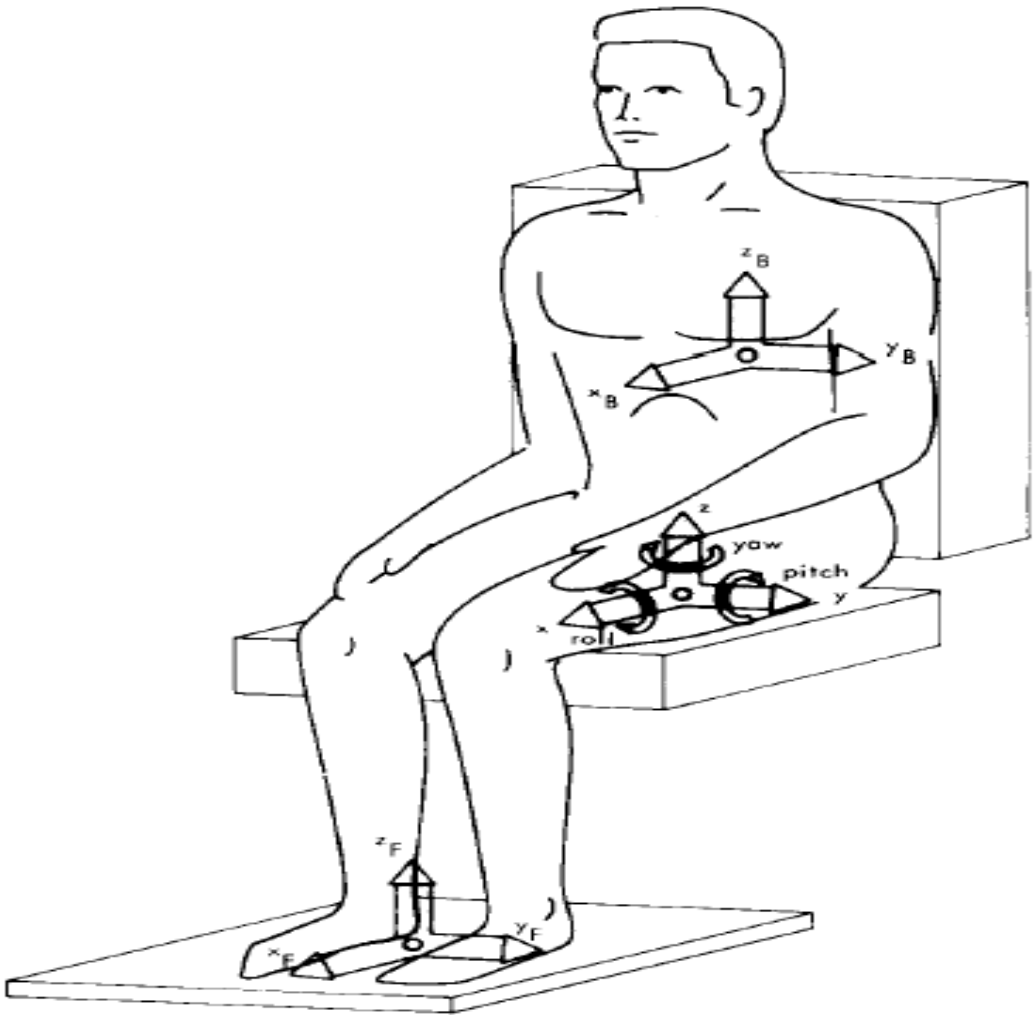

Fig 2.1:-some of the axes along which vibration may enter the human body [17]

2.3 EVALUATION OF VIBRATION EXPOSURES [17]

The evaluation of vibration involves determining the severity of the exposure with respect to one or more human responses. This presumes an adequate understanding of how human responses depend on the magnitude, frequency, direction and duration of vibration.

Knowledge of how some human responses depend on these variables is sufficient to define evaluation procedures which have been shown to be superior to the use of methods which do not take account for this information.

Methods of evaluating vibration with respect to comfort can be offered with some confidence. Means of evaluating vibration with respect to some activities can also be defined--though they may be unsuitable for standardization because of the need to define different methods for each type of task.

Understanding of how human health is affected by vibration is not sufficient to define an evaluation procedure solely by reference to studies directly concerned with health. It is necessary to also utilize knowledge of biodynamic response to vibration and the effects of vibration on comfort.

2.3.1 Vibration frequency

The specification of a method of evaluating vibration with respect health should involve knowledge of how much vibration is required to cause a stated disorder at each frequency of interest-- from, say, 0.5 to 100 Hz.

Clearly, this information is unlikely to be available: experimental studies on volunteers are unacceptable and it is desirable that occupational exposures are prevented from causing the extent of injury or disease necessary for this purpose. The frequency dependence of disorders caused by whole-body vibration is therefore unlikely to be derived solely by evidence from situations where they have occurred.

The frequency dependence of the health effects of vibration could be based on an understanding of the injury mechanisms and biodynamic data. However, while interesting work proceeds in this area, a full understanding of the biodynamic response of the body is far from complete and there are different theories as to how injury may develop.

While not an ideal solution, it currently seems preferable to base the frequency dependence of health effects of whole-body vibration on subjective responses.

Subjective responses partially reflect biodynamic responses and so may also mirror some aspects of the severity of the vibration causing injury--although it is recognized that injury could occur without discomfort.

2.3.2 Vibration axis

The use of subjective response data currently appears to be the only possible basis for formulating frequency dependence for health effects of seat vibration in the horizontal direction, or for other points of contact with the body.

Subjective data also offers the only means for determining the relative importance of vibration in different axes, and the effects of combinations of different frequencies and different axes of vibration.

2.3.3 Vibration duration

The influence of vibration duration has sometimes been expressed by a time-dependent limit. However, it is far more convenient to define a method of determining the cumulative severity of vibration in a 'dose measure'.

Such a procedure should uniquely define how the severities of different durations of exposure should be combined, in addition to stating how severity changes with variations in duration. Again, epidemiological data are insufficient to define the form of this function.

There are useful results from subjective experiments and much practical experience of the general acceptability of various magnitudes and durations of vibration. In the absence of detailed knowledge, the method of forming a “dose” could be consistent with subjective data and should be simple (so as to assist measurements and not falsely imply a sophisticated understanding).

2.3.4 Vibration magnitude

Having decided on the manner in which health effects depend on the frequency and direction of vibration, it might be expected that the effects of different 'quantities' of vibration could be based on epidemiological data.

However, there are currently insufficient data to specify a dose-effect relation for any disorder arising from whole-body vibration. This lack of knowledge should be reflected in any standard offering guidance on the health effects of vibration.

It seems possible to define a procedure for assessing vibration severity which gives numerical values consistent with the impressions of those exposed to vibration. This scale would not define limits, but higher values would cause more discomfort and alarm and can reasonably be expected to be more likely to cause injury.

Some organizations (governments, employers, etc.) may wish to use this scale to institute actions when the severity exceeds certain values. Depending on the action, the selected scale values may be called 'cautionary zones', 'action levels', or 'limits'.

2.4 STANDARDS FOR EVALUATING VIBRATION WITH RESPECT TO HUMAN RESPONSE

2.4.1 International Standard 2631 (1974)

International Standard 2631 (originally published in 1974 and republished with minor changes in 1978 and 1985) was based on complex time-dependent limits which suggested how r.m.s, magnitudes of vibration should decrease with increasing exposure duration from 1 min to 24 h. The ISO 2631 'exposure limits' for selected periods from 1 min to 24 h are illustrated in Fig. 2. The limits are not defined outside the frequency range 1-80 Hz or for durations below 1 min. They are said to be only applicable to motions having a crest factor below about 6--no guidance is given for the assessment of motion in those environments with higher crest factors.

The meaning of the ISO 2631 exposure limit is not defined in relation to any specific injury or disease but the standard indicates that it is at about half the threshold of pain. The one-minute exposure limit will often be considered totally intolerable while many forms of transport exceed the much lower limits for periods in excess of about 8 h without causing any obvious harm.

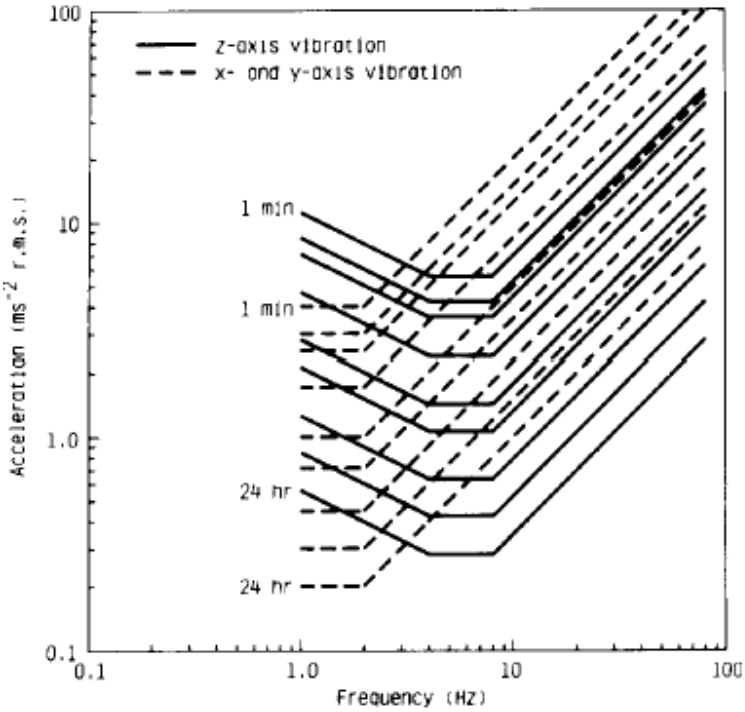

Fig 2.2:-I.S.O 2631 'exposure limits' for durations of 1, 16,25min and 1, 2.5, 4,8,16 and 24 hr

2.4.2 British Standard 6841 (1987)

Recent methods of evaluating vibration employ somewhat different frequency weightings and a simpler time-dependency which can be used to quantify the dose of vibration. The methods may be applied to assess transient motions as well as steady-state and random vibration. The procedure has been included in British Standard 6841 (1987) which was derived from a draft of the revision of International Standard 2631.

The method has been compared with the ISO 2631 method elsewhere. The simplified time-dependency, which is applicable over all durations from fractions of a second to 24 h, is given by a 'fourth power procedure (i.e., motions are equivalent if the fourth powers of their weighted acceleration magnitudes multiplied by their durations are similar). This time-dependency may alternatively be expressed as consisting of 1.5dB reduction in allowable acceleration per doubling of exposure time. The time-dependency can be incorporated in a dose measure.

British Standard 6841 states that high vibration dose values will cause discomfort, pain and injury and those in excess of about 15 $ms^{-1.75}$ will usually cause severe discomfort.

It is reasonable to assume that increased exposure to vibration will be accompanied by increased risk of injury. Fig. 2.3 shows the root-mean-square vibration magnitudes from 0.5 to 80 Hz which are equivalent to these 15 $ms^{-1.75}$ 'action level' for selected exposure durations from 1 s to 24 h. It may be reasonable to use a higher or lower value than 15 $ms^{-1.75}$ when specifying a vibration limit for specific situations.

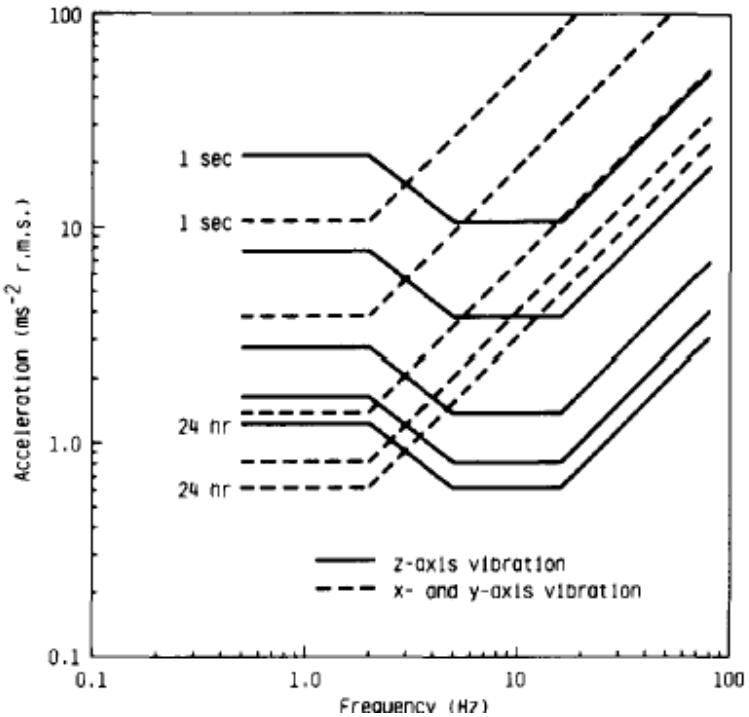

Fig 2.3:-vibration magnitude corresponds to an 'action level' of 15 $ms^{-1.75}$ for duration of 1s, 1m, 1h, 8h and 24h.

Chapter-3

LITERATURE REVIEW

The problem of understanding human response to vibration inputs has interested investigators for many years, as evidenced by a large amount of literature in this area. According to one estimate [3] over 1200 separate studies have been directed to the problem of identifying human response to vibration. These studies fall into three basic categories: comfort studies, impedance studies and transmissibility studies.

One of the major difficulties in modeling and evaluating human body response to vibration arises from the nature of the human body due to variation in size, age, sex and weight. Clearly a living human subject can not be cut open and individual components removed for testing as in any other mechanical structure. Cadavers might be used. However the disadvantages in this case are that it is not possible to duplicate the response obtained from living subjects.

Equations of motion for a model of the human body were developed by Huston [4]. Basically the model consists of an elliptical cylinder representing the torso together with a system of frusta of elliptical cones representing the limbs. They are connected to the main body and each other by hinges and ball and sockets joints. The equations of motion are developed from the principles of classical mechanics. The solution of these equations then provides the displacement and rotation of the main body when the external forces and relative limbs motions are specified.

Bartz and Gionotti [5] discussed the dimensional and inertial properties of human body by formulating a 15-segment model with measurement on the human body.

Garg and Ross [6] presented frequency response of standing human subjected to sinusoidal vibration. The vibratory input was the vertical displacement to the feet, and output was corresponding vertical response of head. They tested twelve subjects (eight males and four females) in the frequency range of 1-50 Hz with small amplitudes. They developed a 16-degree of freedom lumped parameter vibratory model.

A lumped-parameter model of the human body in sitting position is formulated by Muskian [7] which includes the head, vertebral column, upper torso abdomen, thorax viscera, pelvis and legs. The differential equations of motion for the rigid-body

representation of the isolated masses were written for nonlinear spring and dashpots which represented the elasticity and damping, respectively of the physical system. Also included in the equations of motion were coulomb friction forces for modeling sliding surfaces and related muscle contractions in the body and ballistocardiographic and diaphragm muscle forces. Additionally in agreement with the frequency dependency of muscle forces the possibility of frequency dependent damping coefficient was implied.

A Mathematical model for the computational determination of parameter values of anthropometric segments by Hatze [9] which includes model was presented for determining, by computation, the parameter values of anthropomorphic segments from a battery of 242 anthropometric measurements taken directly from the subject. The model consists of 17 segments, includes the shoulders as separate entities, and offers the following advantages over previous models: It subdivides segments into small mass elements of different geometrical structures, thus allowing the shape and density fluctuations of a segment to be modeled in detail. In general, no assumptions were made on segmental symmetry and principal axes transformations are performed whenever necessary. The model differentiates between male and female subjects (exomorphic differences, different density functions and mass distributions), adjusts the densities of certain segmental parts according to the value of a special subcutaneous-fat indicator, and fully accounts for the specificities of pregnancy and obesity. The input data errors are drastically reduced by performing direct anthropometric measurements rather than indirect measurements from photo images; the overall accuracy of the model is better than 3% with a maximum error of about 5%. The features listed above were confirmed by comparing experimentally determined parameter values (volumes, masses, coordinates of mass centroids, principal moments of inertia, and coordinates of segmental origins) with model predictions for four different subjects. The execution time of the computer program executing the model was 0.515 seconds on a CDC Cyber 174 digital computer

Nigam and Malik [13] proposed the use of anthropomorphic models in order to develop a generalized approach for human body vibratory modeling resorting to an experimental program. They developed a linear undamped lumped parameter model on the basis of anthropomorphic model of Bartz and Gionotti [5] in which the segments were identified as ellipsoids. The novel feature of the model was in the determination of masses and stiffness of the various elements of the model. The calculation of the stiffness is based

on the elastic moduli of bones and tissues and geometrical size of the ellipsoid elements. The model was conceived as 15-degree of freedom system.

The frequency response analysis of a human body through analytical modeling has been attempted by Singh N. et. al [14]. A 7- degree-of –freedom spring-mass system has been considered as a representative of male human body in standing posture. A constant harmonic force excitation and constant displacement amplitude excitation acting on the hand position has been considered. The characteristic frequency equations have been formed and frequency response is evaluated by modal matrix method. Eigenvalues and eigenvectors have been computed by Generalized Jacobi Method.

Gupta T.C [15] considered a 15 degree of freedom human model. The back ground available to this work was the approach of Nigam and Malik who proposed that an undamped spring mass vibratory model of the human body can be framed through the anthropomorphic model and using the anthropomorphic data and some elastic properties of bones and tissues. The problem was then to introduce damping in the basic spring mass model.

James and Smith [16] introduced the concept of proportional damping. This is a practical approach to completely uncouple damped free vibration equations. In proportional damping, damping matrix is assumed to be proportional to either the mass matrix or the stiffness matrix K.

Nigam, Singh and Grover [18] had worked on problem of mode shape and frequency response analysis of a human body through analytical modeling. They had considered a 7-degree of freedom spring mass system as a representative of male human body in standing postures.

Nigam S.P. and Malik M. in “mechanical analogue of a human body” presented [19] that the study of engineering aspects of a human body has, lately attracted the attention of engineers, scientists and doctors. Such studies have numerous applications in the field of Bio-Engineering and other allied subjects. It is known that a human body cannot be treated as a lump of mass and it exhibits resonance conditions at certain frequencies. Attempts have been made in the past to formulate a number of spring –mass-dashpot models of multi degree of freedom to facilitate vibration response studies. In this work the natural frequencies of a 7-degree of freedom model of a human body have been evaluated. The dimensional properties of a 50^{th} percentile male were computed from the available

anthropometric data. The stiffness matrix for the model was evaluated and the characteristic frequency equation formed. The computed natural frequencies were found to be within their expected range.

Amirouche et.al [21] used a lumped mass human model to minimize the energy absorption at the feet/hip level when the body is subjected to vertical vibration. Qassem [22] investigated vibrations of a 100kg seated human body on cushions of various mechanical parameters. The vibrations inputs were from (a) steering (b) cushion and(c) a combination of the two. Resonance frequencies and gains of body segments have been found.

`Biodynamic responses to whole body vibrations [22] are usually characterized in terms of transfer functions, such as impedance or apparent mass. Data measurements from subjects are averaged and analyzed with respect to certain attributes (anthropometrics, posture, excitation intensity, etc.). Averaging involves the risk of identifying unnatural vibration characteristics. The use of a modal description as an alternative method is presented and its contribution to biodynamic modeling is discussed. Modal description is not limited to just one biodynamic function: The method holds for all transfer functions. This is shown in terms of the apparent mass and the seat-to-head transfer function. The advantages of modal description are illustrated using apparent mass data of six male individuals of the same mass percentile. From experimental data, modal parameters such as natural frequencies, damping ratios and modal masses are identified which can easily be used to set up a mathematical model. Following the phenomenological approach, this model provided the global vibration behavior relating to the input data. The modal description could be used for the development of hardware vibration dummies. With respect to software models such as finite element models, the validation process for these models can be supported by the modal approach. Modal parameters of computational models and of the experimental data can establish a basis for comparison.

A frequency domain method for estimating the mass stiffness and damping matrices of the model of a structure is presented by Chen [23]. A transformation matrix is obtained from the relationship between the complex and the normal frequency response functions of a structure. The transformation matrix is employed to calculate the damping matrix of the system. The mass and the stiffness matrices are identified from response function by using the least square method.

The vibration to which the human body can be exposed while at work is complex in nature and was obtained by Griffin [26]. It may be composed of various frequencies, occur in several directions and contact the body at more than one point. The vibration will often vary from moment to moment and may contain shocks. The useful evaluation of vibration with respect to human response requires that the manner in which the responses depend on the frequency, direction, duration of the vibration and the occurrence of shocks is adequately taken into account.

Humans are exposed to whole-body vibration in many types of environment that is explained by Mansfield [29]. In almost all cases, the vibration to which the human is exposed comprises of multi-axis vibration, such that vibration occurs in all directions simultaneously. Despite the complex nature of vibration to which humans are exposed in the workplace, almost all laboratory studies investigating the biomechanical response of the person have been completed using single-axis simulators. This paper presents a study whereby 15 male subjects were exposed to single-axis whole-body vibration in the x-, y- and z-directions and dual-axis vibration in the xy-, xz-, and yz-directions using a 6 degree-of-freedom vibration simulator. All vibration magnitudes were $0.4\ \mathrm{ms}^{-2}$ rms in each axis. Acceleration and force was measured in the x-, y-, and z-direction during all trials. Subjects sat in two postures (‘back-on’ and ‘back-off’) on a flat rigid seat. Apparent masses measured using single-axis and dual-axis vibration stimuli showed comparable results; similarly, cross-axis apparent masses (i.e. the ratio of the force in one direction to the acceleration in another direction) were almost identical for the single- and dual-axis vibration stimuli. All results were in agreement with data previously published using single-axis vibration. In most cases, the peaks in the apparent mass and the cross-axis apparent mass occurred at a slightly lower frequency for the dual-axis vibration than for the single-axis vibration. It is hypothesized that this change is due to a nonlinear effect, analogous to that which occurs in increasing the vibration magnitude for single-axis vibration.

Chapter-4

MODELLING OF HUMAN BODY AND EVALUATION OF ANTROPOMETRIC DATA

4.1 Physical Characteristic of Human Body

The human body consists of a hard bony skeleton whose pieces are held together by tough fibrous ligaments and which is embodied in a heavy mass of connective system. Structure of bone is very complex. Most of the supporting membranes are quite flexible. Fluid in body consists of 5 to 6 liters of blood in heart, arteries, veins, capillaries; cerebrospinal fluid surrounding the brain and spinal column and the interstitial fluid. Diameter of these ranges from about 0.001" to 0.01". Approximately 60 to 80 % of the cell is water. Blood is liquid containing nearly 50 % by volume of disc-like red cells, together with white cells. Structure of bone is very complex. There is an outer layer of hard compact material underneath which is a layer of loose sponge like bone so arranged as to produce a maximum of strength for commonly encountered stresses. Density of most soft tissue is between 1.0 kg/m^3 and 1.2 kg/m^3 with fatty tissue being somewhat lighter and bone somewhat heavier.

Most physical data of human body have been derived from analysis of experimental data in which it is assumed that the body is linear and passive. This is an idealization which holds only for very small amplitudes.

The combination of soft tissues and bone in the structure of the body together with the body's geometry exhibits different types of response to vibratory energy depending on the frequency range.

At low frequencies (below approx.100Hz) the body can be described for most purpose as a lumped parameter system; resonance occurs due to interaction of tissue masses with purely elastic structures. At higher frequencies of the body behaves more as a complex distributed parameter system.

It is seen from literature that problems of effect of vibration and shock on human body is directed in the direction of performing the experiments on body parts like head, neck, skull, legs etc. rather than on a complete human body. This is because of intrinsic practical difficulties in such tests in–vivo conditions. Most of the experiments therefore have naturally been confined in-vitro tests.

4.2 Modeling of Human Body

Extensive modeling efforts have been made in the area of Biomechanics based on anthropometric analysis. In order to study human body vibration, it is essential to formulate a mathematical model that duplicates the actual system. The inherent advantage of this approach is that the model parameters can be varied for analysis purposes. Also the model can be subjected to various inputs without endangering human body. A properly matched model would indicate the source of measured human body characteristics such as resonance peaks that would be difficult to determine directly from the subject.

Studying various papers available in the literature, many mathematical models to duplicate human body vibration responses are found. In various studies, there is marked lack of agreement. This is because of different postures and different range of frequency response curve plots by different authors under different study conditions.

4.3 Steps for Model Development

The modeling of human body involves the following steps

1. The segmentation of the body (Fig. 4.1)
2. The evaluation of mass and stiffness values of individual segment
3. Lumping the segments at discrete points and connecting them through mass less spring.
4. Evaluation of the stiffness of the connecting springs of the model via the stiffness values of the individual segments.

The human body is both physically and biologically a system of an extremely complex nature. When looked upon as a mechanical system it contains a number of linear as well as nonlinear elements and the properties are apt to change and are different from person to person. The equation of mass, stiffness, moment of inertia depends on model parameters. As is known human body is very complex system, to determine model parameter one has to simplify this model. To simplify human body model within accuracy range it is necessary to make some assumptions.

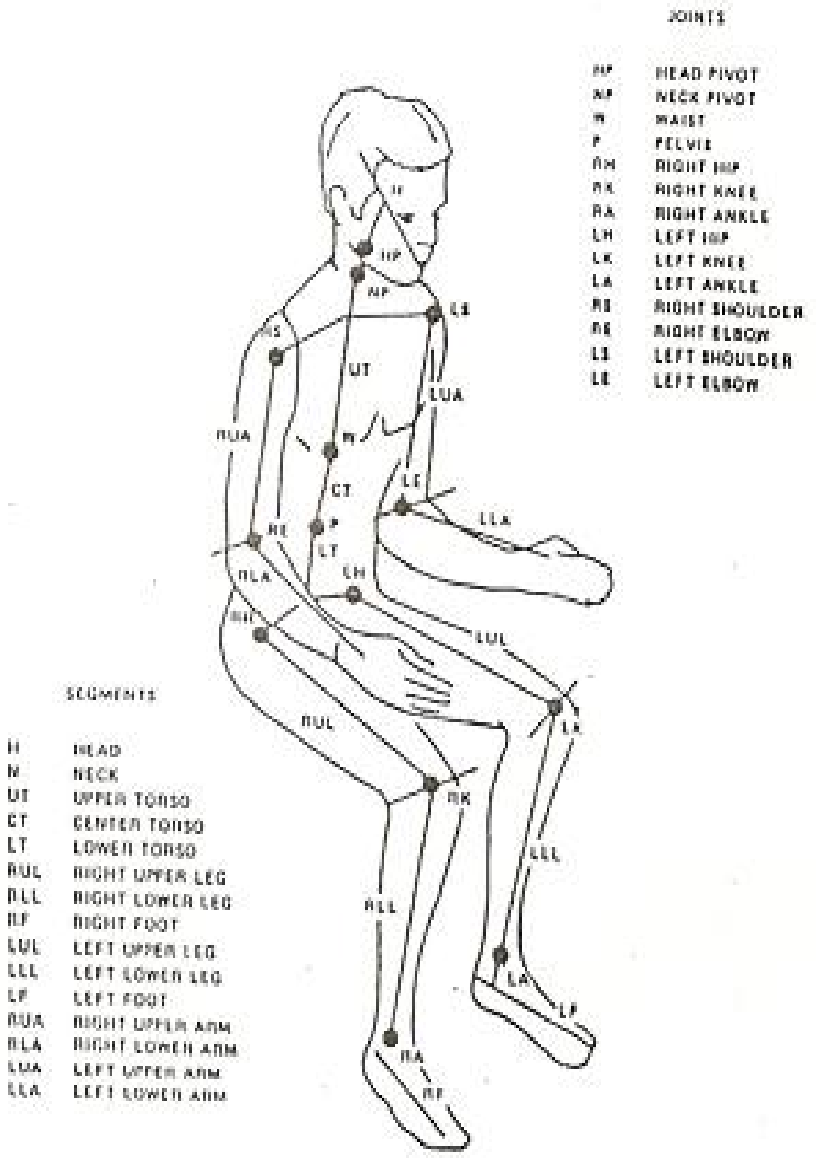

Fig.4.1 Human Body Dynamic Model

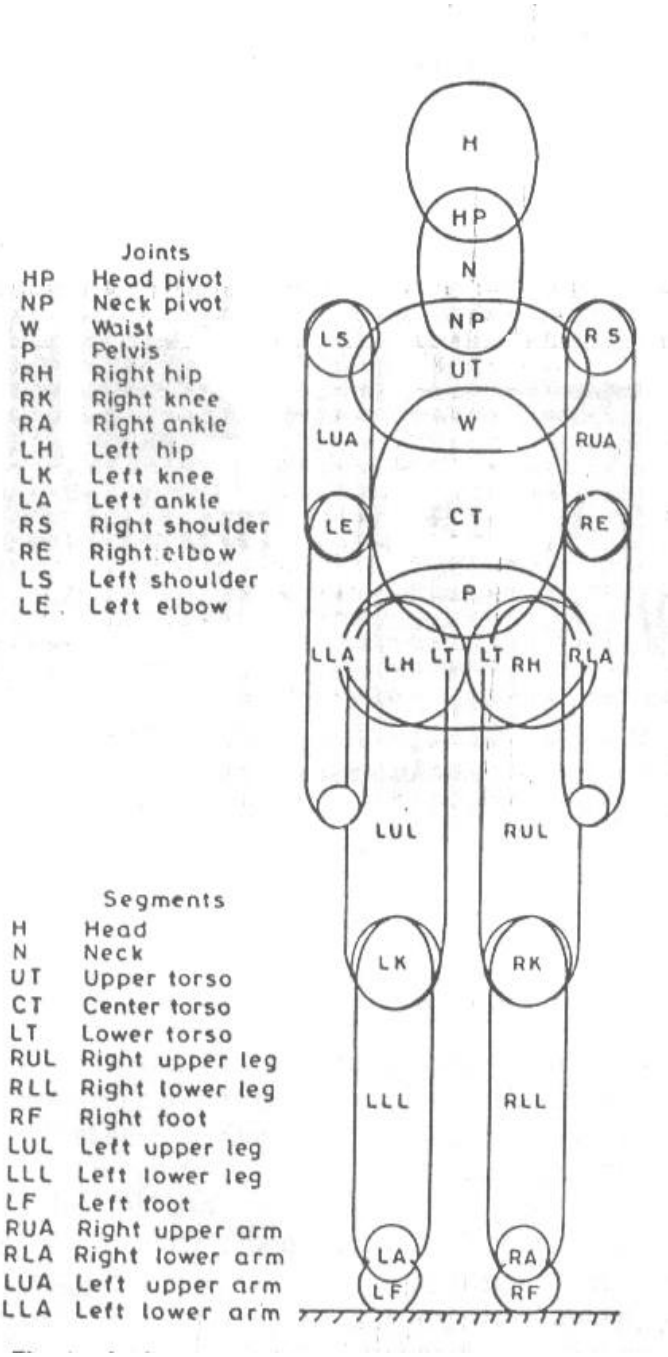

Fig 4.2: Anthropomorphic model of a human body

4.3.1 Assumption for the model development

To proceed further; it is now important to outline the basic assumptions involved in the development of model. These are as follows:

1. For computing the mass dimensional properties, the body segments are considered to be geometrical bodies of known shapes as available in the literature. In the present work an ellipsoidal geometry for each segment has been taken into account, as this geometry resembles with human body segments more closely [5].The human body dynamic model is shown in Fig (4.1) which comprises of 15 body segments with 14 joints.

2. For computing the stiffness of various segments, the ellipsoids are considered to be truncated at ends. This assumption is for the reason that in realistic model, the adjacent ellipsoids must have an overlapping area contact. A model, with point contacting ellipsoids would infect be fragile, while overlapping provides rigidity to the model. Numerically, this assumption is essential to avoid integration value of infinity while calculating stiffness.

3. Though a human body in reality is not a homogenous mass, the bulk average density of different body segments are nearly the same which is taken from the Ref [18] and they are shown in Table4.2. The density of each segment is therefore taken to be the same and equal to the average density of the whole body.

4. The ellipsoids are assumed to be identical and linearly elastic bodies. The assumption of elastic linearity is obviously to account for stiffness linearity of the spring elements. In a human body vibratory model with linear springs and dashpots have been used in literature.

5. Reviewing assumption 4, it is clear that each elastic segment has been joined by another elastic segment by considering the mass acting at the center of gravity of each segment and joined by the series combination of segmental stiffness which is taken from [7]. Segment stiffness and model stiffness have been referred to by letter s and k, respectively. Joint stiffness has not been considered to further simplify the model.

6. Disregarding the effect of all other constituents, the axial deformation in the segments is assumed to be contributed by bones and tissues. The empirical relation has been taken from [6] to get the modulus of elasticity of human body material.

This relation is

$$E=E_bV_b+ E_tV_t \qquad (4.1)$$

Where

E_b= Modulus of elasticity for bones

E_t= Modulus of elasticity for tissues

V_b= Volume fraction of bone

V_t= Volume fraction of tissue.

Elastic modulii of bone and tissue are given in [7]. Which

$E_b= 2.26*10^{11}$ dyen/cm^2 (In S.I unit 2.6 kN/ m^2)

$E_t=7.5*10^9$ dyne/ cm^2 (In S.I unit 7.5 kN/ m^2)

Volume fraction of bone and tissue changes from segment to segment, moreover it changes from one posture to another. Because of non availability of these data following empirical relation is used

$$E = \sqrt[3]{E_b * E_t^2} \qquad (4.2)$$

E=1.08 MN/m^2

4.3.2 Numerical Parameter

Bartz and Gianotti [5] gave geometrical properties of 15 segmented human model having 14 joints (Fig 4.2) of 50th percentile U.S male. Table 4.1 gives the anthropometric data of 50th percentile USA male as reported by Bartz and Gianotti [5].

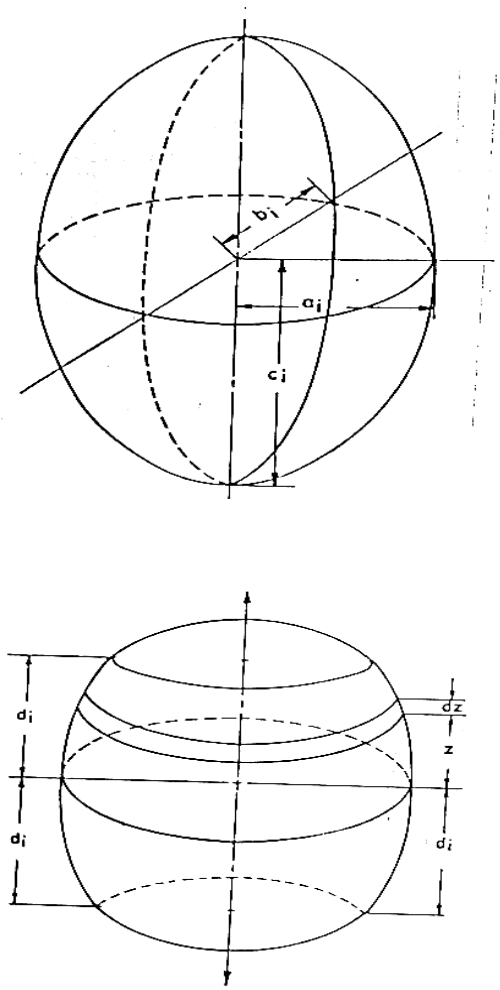

Fig 4.3: (a) An elliptical segment and (b) Truncated ellipsoidal

4.3.3 Evaluation of Mass and Stiffness of the segments

Though a human body is in reality not a homogeneous mass, the bulk (average) densities of different body segments are nearly the same as shown in Table 4.2, which is taken from reference [5]. In a geometrical model each body segment is represented by mean of ellipsoids whose dimensions are known from Table 4.3. Now if it is assumed that weights of all these ellipsoids are proportional to their volumes because specific gravity does not vary much, Table 4.2, the percentage weight of these segments can be fixed up in respect of total body weight.

Table 4.1 Anthropometric Measurements of the 50th Percentile US Man

Dimensional Data	Measurement (cm)
L1 Standing height	168.67
L2 Shoulder height	146.53
L3 Armpit height	136.02
L4 Waist height	108.38
L5 Seated height	92.96
L6 Head length	19.86
L7 Head breadth	15.57
L8 Head to chin height	23.24
L9 Neck circumference	37.95
L10 Shoulder breadth	46.20
L11 Chest depth	23.32
L12 Chest breadth	32.89
L13 Waist depth	21.51
L14 Waist breadth	28.22
L15 Buttock depth	23.19
L16 Hip breadth, standing	35.43
L17 Shoulder to Elbow length	37.54
L18 Forearm-hand length	48.69
L19 Biceps circumference	32.52
L20 Elbow circumference	31.42
L21 Forearm circumference	29.28
L22 Wrist circumference	17.86
L23 knee height, seated	53.14
L24 Thigh circumference	50.52
L25 Upper leg circumference	37.24
L26 Knee circumference	36.20
L27 Calf circumference	33.32
L28 Ankle circumference	21.06
L29 Ankle height, outside	6.91
L30 Foot breadth	9.35
L31 Foot length	25.40

Table 4.2 Average Body Segment Specific Gravity

S.No.	Segment	Specific Gravity
1	Head, Neck	1.111
2	Upper Torso, Central Torso	1.031
3	Upper arm	1.081
4	Lower arm	1.122
5	Upper leg	1.069
6	Lower leg	1.095
7	Foot	1.100

The densities of each segment are therefore taken to be the same and equal to the average density of the whole body. Therefore the mass of an i^{th} segment may be expressed as

$$M_i = \frac{M * V_i}{\sum_{j=1}^{n} V_j} \tag{4.3}$$

Where

Vi = Volume of i^{th} segment = $\pi * a_i * b_i * c_i$

a_i, b_i, c_i are the semi axes of the ellipsoid.

n = Total number of segments

M = Total body mass

4.3.4 Moment of Inertia of the segments

The calculation of moment of inertia of each ellipsoidal segment was performed using the expressions, which are taken from. [5]

$$I_{ix} = \frac{M_i}{5}(b_i^2 + c_i^2) \tag{4.4a}$$

$$I_{iy} = \frac{M_i}{5}(a_i^2 + c_i^2) \tag{4.4.b}$$

$$I_{iz} = \frac{M_i}{5}(a_i^2 + b_i^2) \tag{4.4c}$$

Where

a_i, b_i, c_i, are semi-axes of i^{th} ellipsoidal segment in x, y, z axes respectively and Mi is the mass of that particular segment.

Table 4.3 Formulae for statistical dimensions of ellipsoids representing Body segments

Body Segment	Mass elements	Formulae		
		a_i	b_i	c_i
Head (H)	M1	$L_7/2$	$L_7/2$	$L_6/2$
Neck (N)	M2	$L_8/2\pi$	$L_8/2\pi$	$(L_1-L_2-L_6)/2$
Upper torso (UT)	M3	$L_{12}/2$	$L_{11}/2$	$L_{17}/2$
Central torso (CT)	M8	$L_{14}/2$	$L_{13}/2$	$(L_{17}+L_{18})/4$
Lower torso	M9	$L_{16}/4$	$L_{15}/2$	$L_{18}/4$
Upper arms (RUA,LUA)	M4,M5	$L_{19}/2\pi$	$L_{19}/2\pi$	$L_{19}/2$
Lower arms (RLA,LLA)	M6,M7	$L_{21}/2\pi$	$L_{21}/2\pi$	$L_{18}/2$
Upper legs (RUL,LUL)	M10,M11	$L_{25}/2\pi$	$L_{25}/2\pi$	$(L_{21}-L_{17}-L_{23})/2$
Lower legs (RLL,LLL)	M12,M13	$L_{27}/2\pi$	$L_{27}/2\pi$	$(L_{23}-L_{29})/2$
Feet (RF,LF)	M14,M15	$L_{30}/2$	$L_{31}/2$	$L_{29}/2$

4.3.5 Spring stiffness of a segment

Consider a body segment in uniaxial loading as shown in Fig 4.4. The change in given axial length is given by

$$\delta I = \int_{-C_i}^{C_i} \frac{F}{E A(z)} * dz$$

The axial stiffness of the segment then becomes,

$$S_i = \frac{F}{\delta I} = \frac{1}{\int_{-c_i}^{c_i} \frac{1}{E\,A(z)}\,.\,dz} = \frac{E}{I_i}$$

Where

$$I_i = \int_{-c_i}^{c_i} \frac{1}{A(z)} * \quad dz \qquad (4.5)$$

E is the axial elastic modulus of elasticity given by relation (4.2).

The expression of stiffness for ellipsoidal segment shape is given as follows,

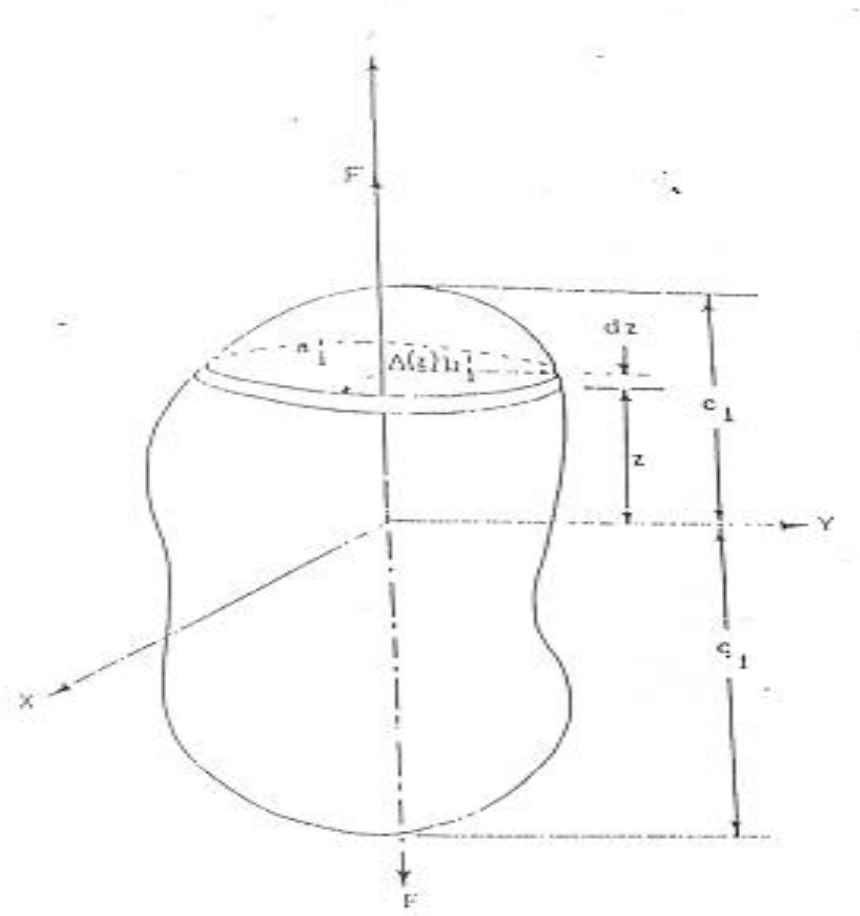

Fig 4.4 A body segment uniaxial loading

Ellipsoids:

To find Ii, the equation of ellipsoid is

$$\frac{X^2}{a_i^2} + \frac{Y^2}{b_i^2} + \frac{Z^2}{c_i^2} = 1$$

Where a_i, b_i, c_i, are semi-axes of ellipsoid. If a'_i, b'_i, c'_i, are semi-axes at any transverse section of the ellipsoid shown in fig. 4.3 (a), then $A(z)= \pi * a'_i * b'_I$, and also

$$\frac{b_i'^2}{b_i^2} = 1 - \frac{Z^2}{c_i^2}$$

$$\Rightarrow \quad b'_i = b_i \sqrt{1 - \frac{Z^2}{c_i^2}}$$

Similarly,

$$a'_i = a_i \sqrt{1 - \frac{Z^2}{c_i^2}}$$

Hence,

$$A(z) = \frac{\pi a_i b_i}{c_i^2}(c_i^2 - z^2)$$

From Equation (4.4)

$$I_i = \int_{-c_i}^{c_i} \frac{c_i^2}{\pi a_i b_i (c_i^2 - z^2)}.dz$$

$$= \frac{c_i^2}{\pi a_i b_i} \int_{-c_i}^{c_i} \frac{1}{(c_i^2 - z^2)}.dz$$

$$= \frac{c_i}{2\pi a_i b_i} log \left. \frac{c_i + z}{c_i - z} \right|_{-c_i}^{c_i}$$

The above integral is obviously undefined at the lower and upper limits of integration i.e. at $Z=\pm c_i$. However, the integral may be evaluated if the ellipsoids are assumed to be truncated at the two ends. Although this assumption arises as a mathematical requirement, it complies with the physical state also. In an anthropomorphic model with segment represented by ellipsoids, the contact between adjacent segments cannot be a point contact. In fact such a model would be fragile and in a real model the contact between adjacent segments should be an area contact. This purpose is served by taking the ellipsoids to be truncated at the ends.

Taking the truncated length of the ellipsoid to be 2 d_i ($d_i < c_i$) (Fig. 4.3(b)), the integral becomes

$$I_i = \frac{c_i}{\pi a_i b_i} log \left(\frac{c_i + d_i}{c_i - d_i} \right)$$

$$S_i = \frac{E}{I_i}$$

$$S_i = \frac{E \pi a_i b_i}{c_i log \left(\frac{c_i + d_i}{c_i - d_i} \right)} \quad (4.6)$$

Nigam and Malik [8] have used ellipsoidal segment in their vibratory model and truncation of 5% at both the ends i.e. d_i=0.95 c_i. In this work also same truncation factor is assumed, there fore segmental stiffness can be expressed as

$$S_i = 0.857524 \frac{E a_i b_i}{c_i}$$

Substituting the value of E from equation 4.2, we get

$$S_i = 929 \frac{a_i b_i}{c_i} kN/m^2 \quad (4.7)$$

The values of semi axes of ellipsoidal segment can be calculated by using Table 4.3 and table 4.1. Using the values of semi-axes, equation 4.3, and 4.7. The mass and stiffness values of each segment have been obtained and tabulated in Table 4.4

Table 4.4 Mass and Stiffness Values of the Ellipsoidal Segments

(50^{th} Percentile U.S. Male)

Truncation Factor $t_r = 0.05$

Segment Elastic modulus, $E = \sqrt[3]{E_b * E_t^2}$ =1.08 MN/m^2

Seg no.	**Segment Designation**	**Semi-axes of Ellipsoids computed from table 4.3**			**Mass of the segment M(kg) from Eq.4.2**	**Stiffness of the segment**	
		a_i (cm)	b_i (cm)	c_i (cm)		Designation	S_i From Eq. 4.6 (kN/m)
1	HEAD	7.785	7.785	9.931	3.310	S_1	680
2	NECK	6.020	6.020	1.130	0.214	S_2	3,576
3	U.TORSO	16.450	11.660	9.385	9.390	S_3	2279
8	C.TORSO	14.110	10.760	21.550	17.067	S_8	785.82
9	LTORSO	8.858	11.660	12.110	6.491	S_9	941.86
4,5	U.ARM	5.239	5.239	18.770	2.687	S_4, S_5	163
6,7	L.ARM	4.629	4.629	24.330	2.720	S_6, S_7	98.22
10,11	U.LEG	5.926	27.930	5.926	5.116	S_{10}, S_{11}	140.43
12,13	L.LEG	5.304	5.304	23.110	3.391	S_{12}, S_{13}	135.7
14,15	FEET	4.674	12.700	6.909	1.139	S_{14}, S_{15}	958

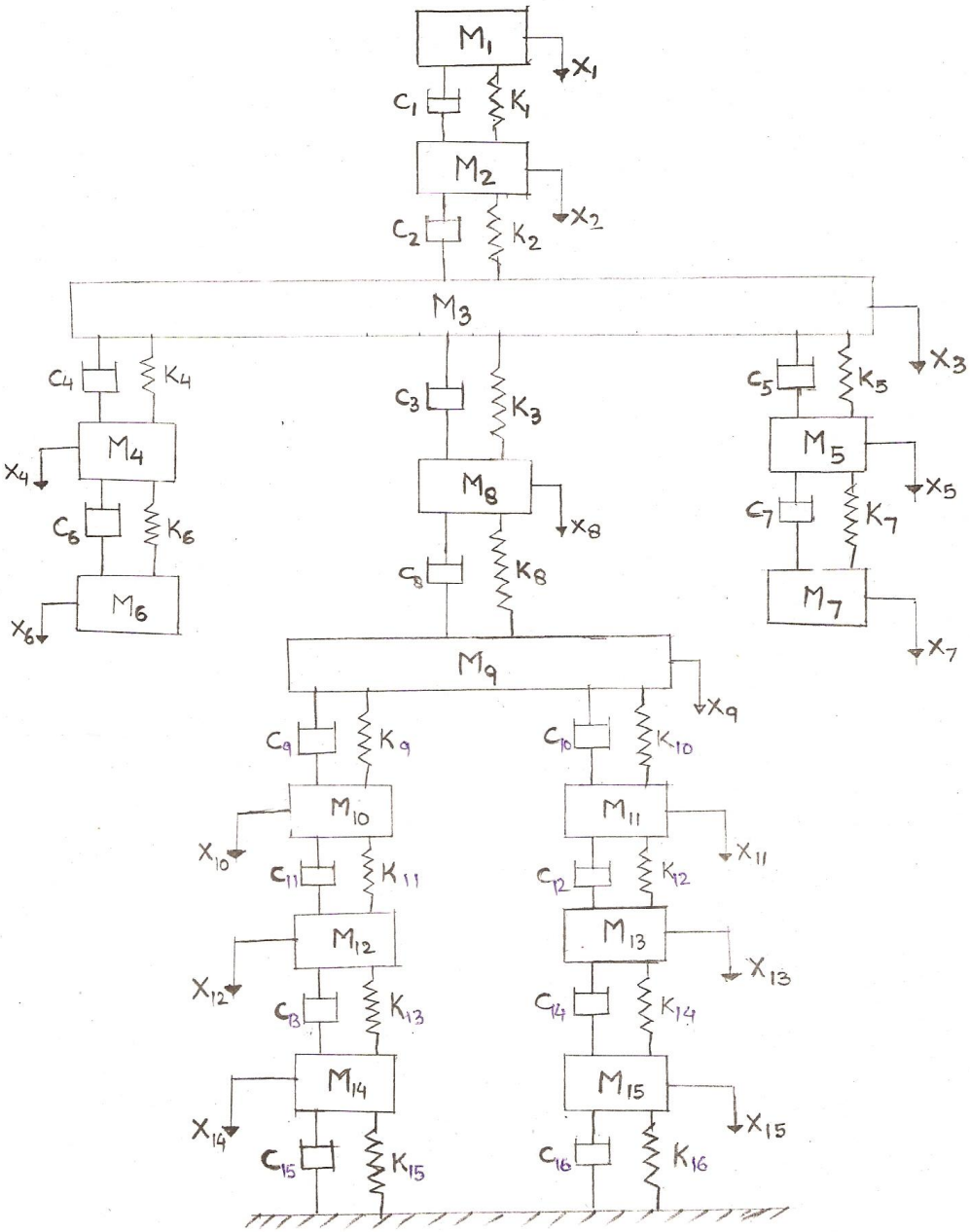

Fig 4.5 Vibratory model of a human

4.4 VIBRATORY MODEL

Although a human body is a completely unified organic system, it just can not be treated as a lump of mass. When subjected to external excitations it exhibits resonances at discrete frequency levels as it should, because of its being basically an elastic system. To analyse the mechanical response of a human body, one must have the information about the constitutive mechanical properties. From a vibration point of view a human body should be treated as a continuous system which is indeed a formidable task. The lumped parameter modeling is perhaps a relatively accessible task and has in fact been the approach used by most authors. However, unlike the vibratory models of the machine and structures, the vibratory model of a human body is at best a mathematical approximation and can never be considered to be its true representative. The reason being that human body has an inherently reflexive nature which always reacts through its nervous system to any adverse environment. This active nature is perhaps impossible to be accounted for in a model which would therefore be always a passive model.

The number of mass elements in the vibratory model equals the number of segments in anthropomorphic model. The various segments as identified by Bartz and Gianotti are shown in Fig 4.1. Bartz and Gianotti approximated the body segment by ellipsoids (Fig 4.2). Values of semi axes of ellipsoidal segment can be calculated by using Table 4.1 and table 4.3. Using values of semi axes, eq.4.2 and eq.4.4 one can find mass and stiffness of segment are given in table 4.4. Spring, dashpot distribution for standing posture is shown in Fig 4.5

For any segment, the stiffness of upper half and lower half from the center of gravity of the segment will be equal. Numerically the value of half of the spring will be twice the stiffness of the segment; similar is true for viscous damping coefficient. A general rule is that series combination is taken when subdividing the length of segment and parallel combination is used when subdividing the area normal to the loading. One can find model stiffness K for vibratory model shown in Fig. 4.5. Values of model stiffness K are given in Table 4.5. Formulae for model damping are given in Table 4.6.

Table 4.5 Stiffness of the spring elements

Spring element Designation	Formulae	Numerical Value kN/ m^2
K_1	S_1	680.5
K_2	$S_2 S_3 / (S_2 + S_3)$	1392
K_3	$S_3 S_8 / (S_3 + S_8)$	584.2
K_4	$S_3 S_4 / (S_3 + S_4)$	152.1
K_5	$S_3 S_5 / (S_3 + S_5)$	152.1
K_6	S_6	98.1
K_7	S_7	98.1
K_8	$S_8 S_9 / (S_8 + S_9)$	555.1
K_9	$S_9 S_{10} / (S_9 + S_{10})$	130.5
K_{10}	$S_9 S_{11} / (S_9 + S_{11})$	130.5
K_{11}	$S_{10} S_{12} / (S_{10} + S_{12})$	68.9
K_{12}	$S_{11} S_{13} / (S_{11} + S_{13})$	68.9
K_{13}	$S_{12} S_{14} / (S_{12} + S_{14})$	118.86
K_{14}	$S_{13} S_{15} / (S_{13} + S_{15})$	118.86
K_{15}	S_{14}	958

Table 4.6 Damping constants of the Vibratory Model

Damping element Designation	Formulae
C_1	$2\beta_1\beta_2/(\beta_1+\beta_2)$
C_2	$2\beta_2\beta_3/(\beta_2+\beta_3)$
C_3	$2\beta_3\beta_8/(\beta_3+\beta_8)$
C_4	$2\beta_3\beta_4/(\beta_3+\beta_4)$
C_5	$2\beta_3\beta_5/(\beta_3+\beta_5)$
C_6	$2\beta_4\beta_6/(\beta_4+\beta_6)$
C_7	$2\beta_5\beta_7/(\beta_5+\beta_7)$
C_8	$2\beta_8\beta_9/(\beta_8+\beta_9)$
C_9	$2\beta_9\beta_{10}/(\beta_9+\beta_{10})$
C_{10}	$2\beta_9\beta_{11}/(\beta_9+\beta_{11})$
C_{11}	$2\beta_{10}\beta_{12}/(\beta_{10}+\beta_{12})$
C_{12}	$2\beta_{11}\beta_{13}/(\beta_{11}+\beta_{13})$
C_{13}	$2\beta_{12}\beta_{14}/(\beta_{12}+\beta_{14})$
C_{14}	$2\beta_{13}\beta_{15}/(\beta_{13}+\beta_{15})$
C_{15}	$2\beta_{14}$
C_{16}	$2\beta_{15}$

Where

β = Damping coefficient of the segment

Chapter-5

DAMPING OF THE VIBRATORY MODEL

5.1 EVALUATION OF DAMPING COEFFICIENTS OF THE SEGMENT

When a body vibrates in a fluid medium it will experience a resistance due to the viscosity of the fluid. This type of damping is called viscous damping.

It is represented by a dash pot as shown in Fig 5.1. It is called dash pot or damper. Here the piston reciprocates in a cylinder which is filled with a fluid and there will be a clearance between the piston and the cylinder.

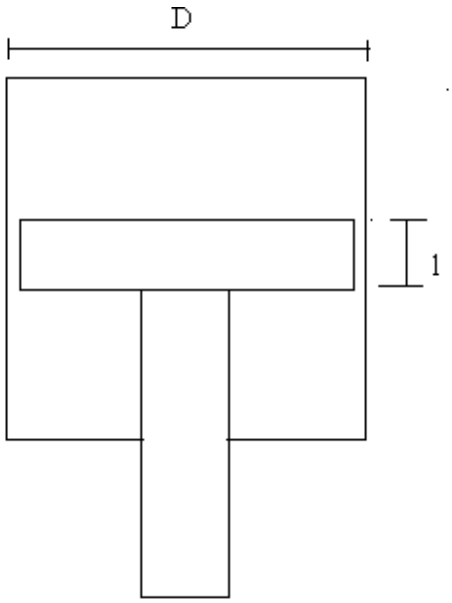

Fig 5.1 Fluid dash pot system

Where

l = length of piston

e = clearance between the piston and cylinder

D = diameter of the cylinder

The major sources of damping depend on both the system and the environment. The most common sources are

i) Drag between a moving body and its fluid environment

ii) Damping produced by the pressure flow of the fluid through the clearance space as a result of piston displacement.

iii) Damping resistance due to the pressure difference on the two sides of the piston. This pressure difference is caused by the restriction to fluid flow due to piston motion.

If the clearance between the piston and the cylinder is small, the first two components of the damping are negligible and the total damping is due to third component only.

The damping coefficients of the individual segments are established in terms of the diameter, length of segments and coefficient of viscosity of the fluids. [27]

$$\beta_i = \frac{12\mu}{\pi} X \frac{A_s^2 l}{D_m e^3} \qquad (5.1)$$

Where

β_i = Viscous damping coefficient of i^{th} segment

μ = Effective coefficient of viscosity of blood and synovial fluid

A_s = Area of the Segment

l = Length of the segment

D_m = Mean diameter of the segment

e = Clearance

The dimensional data of each segment has been given in Table 4.1. From these data diameter and length of each segment has been calculated. This is given in Table 5.1.

Using values in Table 5.1 and Eq.5.1, one can find damping coefficient of individual segment. To calculate the damping coefficient within range of experimental values identified by T.C.Gupta it is necessary to make some assumptions, as regards to the following:.

(i) Coefficient of viscosity of the blood

(ii) Clearance between the piston and cylinder

(iii) Length of the piston

Table 5.1 Formulae for geometrical dimensions of the body segment

Body segment	Diameter of the segment (D_i)	Length of the segment L	D_i (cm)	L (cm)
H	L_7	L_6	15.57	19.86
N	L_9/π	L_1- L_2- L_6	12.08	2.28
UT	L_{11}	$L_{17}/4$	23.32	9.378
RUA,LUA	$\left(\frac{L_{20}}{\pi}+\frac{L_{19}}{\pi}\right)/2$	L_{17}	10.24	37.54
RLA, LLA	$\left(\frac{L_{20}}{\pi}+\frac{L_{22}}{\pi}\right)/2$	L_{18}	7.84	48.69
CT	L_{13}	L_{17} + $L_{18}/4$	21.51	21.5
LT	L_{15}	$L_{18}/4$	23.19	12.11
RUL, LUL	$\left(\frac{L_{25}}{\pi}+\frac{L_{26}}{\pi}\right)/2$	L_2- L_{17}- L_{23}	11.68	55.85
RLL, LLL	$\left(\frac{L_{26}}{\pi}+\frac{L_{28}}{\pi}\right)/2$	L_{23}- L_{29}	8.65	46.22
RF, LF	L_{30}	L_{31}	9.35	25.40

The damping ratio of i^{th} segment is given by

$$\xi_i = \frac{\beta_i}{2\sqrt{S_i M_i}} \qquad (5.2)$$

Where

β_I = Damping constant of the i^{th} segment (N-s/m)
ξ_i =Damping ratio of the i^{th} segment
S_i = Stiffness of the segment (N/m)
M_i= Mass of the segment

Certain range of damping ratio of the segments has been identified by T.C.Gupta [15] and Garg and Ross [6]. This has been given in Table 5.2 and 5.3

Table 5.2 Range of damping ratio values for different body segment (Gupta)

BODY SEGMENT	ξ_i
Foot and legs	1 –1.5
Lower torso	0.5 –1.0
Central torso	0.01 –0.2
Upper torso	0.002- 0.015
Hands	0.001 – 0.01
Neck	0.015
Head	0.004

Table 5.3 Range of damping ratio values for different body segment (Garg & Ross)

BODY SEGMENT	ξ_i
Foot and legs	0.2939-0.5615
Lower torso	0.5
Central torso	0.0686
Upper torso	0.6339
Hands	0.2668-0.5014
Neck	0.00958
Head	0.0092

5.2 VISCOSITY OF BLOOD

Human blood is a suspension of particles in a complex aqueous continuous phase. This continuous phase is called plasma. Blood is neither a homogenous fluid nor Newtonian fluid. Plasma in isolation may be considered as Newtonian with viscosity of about 1.2 times that of water. The constitutive equation proposed for whole blood is taken from [20].

$$\mu_b = \frac{\tau}{e^n} \qquad (5.3)$$

Where

μ_b is the coefficient of viscosity of blood,

τ is the shear stress and e is the strain rate

This is found to hold good for strain rates between 5 and 200 sec^{-1} with n having a value between 0.68 to 0.80. At low shear stress, red cells from aggregates in the from of rouleaux which are stacks of red cells in the shape of a roll of coins. At some finite stress, which is usually small and order of 0.0005 dyne/cm^2 ($5*10^{-5}$ N/m^2), the aggregate is disrupted and blood begins to flow. [20]

There are other fluids also, however, for blood flows, Newtonian, Herschell-bulkley fluid and Casson fluid have been found especially useful. Plasma in isolation may be considered Newtonian with a viscosity of 3cp. For computing the damping coefficients of individual segments, the blood is considered here to be Newtonian fluid. For whole human blood one can assume viscosity as 3cp.

5.3 EVALUATION OF CLEARANCE AND LENGTH OF THE SEGMENT

For evaluating the damping coefficients of the dashpots in the model as explained in section 5.1. It is first necessary to identify the damping ratios of individual body segments. The range of damping ratios of the segments has been given in Table 5.2. The damping ratios, whatever identified in T.C. Gupta's [15] work to be assessed on the basis of the frequency response of model against the experimental response.

Using equation (5.2) the damping ratios of the individual segments obtained by changing the clearance and length of various body segments. The results of some of these computations are shown in Table 5.4 the experimental range of damping ratios of the segments has been given in Table 5.2. From the Table 5.4, the most appropriate set of clearance and length of the segments ranges were found by comparing these damping ratio values with the experimental ranges shown in Table 5.2 and tabulated in Table 5.4. Using values of clearance, length of the individual segments, calculated values of damping coefficients of individual segment are given in Table 5.5. Also the damping constants of vibratory model (Fig 4.5) are obtained from the formulae of Table 4.6. These values have been given in Table 5.6.

Table5.4 Effect of clearance and length of the segments on damping ratio

Clearance (e=X%D)	Length of the piston(l=Y%L)	Damping Ratio values of different body segment									
X	Y	**H**	**N**	**UT**	**UA**	**LA**	**CT**	**LT(HIP)**	**UL**	**LL**	**F**
1	1	0.0159	0.0034	0.01082	0.0833	0.2453	0.02003	0.00271	0.4423	0.1928	0.1755
	3	0.0567	0.0104	0.02164	0.2499	0.7361	0.02164	0.00813	1.327	0.5775	0.5265
	5	0.0945	0.0149	0.03246	0.4166	1.2261	0.10001	0.01356	2.2117	0.9625	0.8976
	7	0.1323	0.0243	0.04328	0.5832	1.7176	0.1402	0.0189	3.0964	1.3475	1.2287
	9	0.1701	0.0313	0.0541	0.7499	2.2083	0.1803	0.0244	3.9811	1.7325	1.5397
3	1	0.0007	0.0001	0.0004	0.0031	0.00927	0.00075	0.0001	0.0167	0.0072	0.0066
	3	0.0021	0.0004	0.0008	0.0094	0.02767	0.00227	0.0003	0.0501	0.0218	0.0199
	5	0.0035	0.0006	0.000122	0.0157	0.04637	0.00378	0.00051	0.0836	0.0363	0.0331
	7	0.005	0.0009	0.00163	0.022	0.06492	0.0052	0.00071	0.117	0.0509	0.0464
	9	0.0064	0.0011	0.00204	0.0283	0.08347	0.0068	0.00092	0.1504	0.0654	0.0597
5	1	0.0002	0.00009	0.00009	0.00069	0.00204	0.00016	0.000023	0.00368	0.0016	0.00146
	3	0.0005	0.00016	0.00016	0.00208	0.00613	0.0005	0.000065	0.011063	0.0048	0.00439
	5	0.0007	0.00027	0.00027	0.00347	0.0102	0.00083	0.000113	0.01843	0.008	0.00731
	7	0.0011	0.00036	0.00036	0.00486	0.0143	0.00116	0.000158	0.0258	0.0112	0.0102
	9	0.0014	0.00045	0.00045	0.00625	0.0184	0.0015	0.000203	0.03319	0.0144	0.01317
7	1	0.0001	0.000011	0.000011	0.000259	0.00076	0.000062	0.000008	0.0007	0.000597	0.00059
	3	0.0003	0.000032	0.000032	0.000776	0.00228	0.000187	0.000025	0.0022	0.0017	0.0019
	5	0.0004	0.000054	0.000054	0.00129	0.0038	0.000311	0.000042	0.0038	0.00298	0.00298
	7	0.0006	0.000076	0.000076	0.00181	0.00533	0.000435	0.000059	0.0053	0.00418	0.00418
	9	0.0008	0.000097	0.000097	0.00232	0.00685	0.00056	0.00232	0.0068	0.00537	0.00537

l=length of piston

L=length of the segment,

D=diameter of the segment

For computing the damping coefficients of individual segments in present work the following set of clearance and length of the piston are used

Table 5.5 Range of clearance values and length for different body segments

Body segments	Clearance(Cl)	Piston length (l)
H	7% of D	6% of L
Ne	6% of D	6% of L
UT &CT	6% of D	6% of L
LT	1% of D	6% of L
HANDS	9% of D	4% of L
FOOT and LEGS	4% of D	4% of L

L=length of the individual segment, D=diameter of the individual segment

Table5.6. Damping coefficients and Damping constants of body segments

Damping coefficients (N-sec/m)		Damping constants (N-sec/m)	
Symbol	Values	Symbol	Values
β_1	4.10	C_1	4.80
β_2	5.80	C_2	7.6
β_3	11.00	C_3	6.50
β_4	3.00	C_4	3.30
β_5	3.00	C_5	3.30
β_6	10.60	C_6	4.68
β_7	10.60	C_7	4.68
β_8	28.73	C_8	55.55
β_9	835.25	C_9	699.71
β_{10}	2155.85	C_{10}	699.71
β_{11}	2155.85	C_{11}	1034.40
β_{12}	680.44	C_{12}	1034.40
β_{13}	680.44	C_{13}	759.07
β_{14}	858.26	C_{14}	759.07
β_{15}	858.26	C_{15}	1716.52
		C_{16}	1716.52

CHAPTER-6

MATHEMATICAL ANALYSIS AND COMPUTATIONAL PROCEDURE

Development of vibratory model has been discussed in pervious chapter. In this chapter mathematical analysis of the vibratory model has been carried out. To determine the frequency response of the model, equations of motion are required.

6.1 Evaluation of Mass, Stiffness and Damping Matrices

It is 15 degree of freedom system. It will require 15 equations of motion to define system completely. These equations can be derived by the application of D'Alemberts principle. The equations are

$$M_1\ddot{X}_1 = C_1(\dot{X}_2 - \dot{X}_1) + K_1(X_2 - X_1)$$

$$M_2\ddot{X}_2 = -C_1(\dot{X}_2 - \dot{X}_1) + C_2(\dot{X}_3 - \dot{X}_2) + K_2(X_3 - X_2) - K_1(X_2 - X_1)$$

$$M_3\ddot{X}_3 = -C_2(\dot{X}_3 - \dot{X}_2) + C_4(\dot{X}_4 - \dot{X}_3) + C_5(\dot{X}_5 - \dot{X}_3) + C_3(\dot{X}_8 - \dot{X}_3) + K_3(X_8 - X_3) + K_4(X_4 - X_3) + K_5(X_5 - X_3) - K_2(X_3 - X_2)$$

$$M_4\ddot{X}_4 = C_6(\dot{X}_6 - \dot{X}_4) - C_4(\dot{X}_4 - \dot{X}_3) + K_6(X_6 - X_4) - K_4(X_4 - X_3)$$

$$M_5\ddot{X}_5 = C_7(\dot{X}_7 - \dot{X}_5) - C_5(\dot{X}_5 - \dot{X}_3) + K_7(X_7 - X_5) - K_5(X_5 - X_3)$$

$$M_6\ddot{X}_6 = -C_6(\dot{X}_6 - \dot{X}_4) - K_6(X_6 - X_4)$$

$$M_7\ddot{X}_7 = -C_7(\dot{X}_7 - \dot{X}_5) - K_7(X_7 - X_5)$$

$$M_8\ddot{X}_8 = -C_3(\dot{X}_8 - \dot{X}_3) + C_8(\dot{X}_9 - \dot{X}_8) + K_8(X_9 - X_8) - K_3(X_8 - X_3)$$

$$M_9\ddot{X}_9 = -C_8(\dot{X}_9 - \dot{X}_8) + C_9(\dot{X}_{10} - \dot{X}_9) + C_{10}(\dot{X}_{11} - \dot{X}_9) + K_9(X_{10} - X_9) + K_{10}(X_{11} - X_9) - K_8(X_9 - X_8)$$

$$M_{10}\ddot{X}_{10} = -C_9(\dot{X}_{10} - \dot{X}_9) + C_{11}(\dot{X}_{12} - \dot{X}_{10}) + K_{11}(X_{12} - X_{10}) - K_9(X_{10} - X_9)$$

$$M_{11}\ddot{X}_{11} = -C_{10}(\dot{X}_{11} - \dot{X}_9) + C_{12}(\dot{X}_{13} - \dot{X}_{11}) + K_{12}(X_{13} - X_{11}) - K_{10}(X_{11} - X_9)$$

$$M_{12}\ddot{X}_{12} = -C_{12}(\dot{X}_{12} - \dot{X}_{10}) + C_{13}(\dot{X}_{14} - \dot{X}_{12}) + K_{13}(X_{14} - X_{12}) - K_{12}(X_{12} - X_{10})$$

$$M_{13}\ddot{X}_{13} = -C_{12}(\dot{X}_{13} - \dot{X}_{11}) + C_{14}(\dot{X}_{15} - \dot{X}_{13}) + K_{13}(X_{15} - X_{13}) - K_{12}(X_{13} - X_{11})$$

$$M_{14}\ddot{X}_{14} = -C_{13}(\dot{X}_{14} - \dot{X}_{12}) + C_{15}\dot{X}_{14} + K_{15}X_{14} - K_{13}(X_{14} - X_{12})$$

$$M_{15}\ddot{X}_{15} = -C_{14}(\dot{X}_{15} - \dot{X}_{13}) + C_{16}\dot{X}_{15} + K_{16}X_{15} - K_{14}(X_{15} - X_{13})$$

In matrix form these equations can be written as

$$[M]\{\ddot{X}\} + [C]\{\dot{X}\} + [K]\{X\} = [F]\sin\omega t \quad \ldots\ldots\ldots\ldots\ldots 6.1$$

Where [M], [C] and [K] are 15x15 matrices as listed in tabular form. All the elements of mass matrix are zero except diagonal elements which are placed in the same order as given in Table 4.4. The elements of damping and stiffness matrices were obtained from equation of motion given above. [F] is the 15x1 column matrix. All the elements of force matrix are zero except 14th and 15th elements. The 14th and 15th elements are forces on left foot and right foot respectively and in the case of hand all the elements of force matrix are zero except 6th and 7th elements. The 6th and 7th elements are forces on left hand and right hand respectively

6.2 Determination of response by matrix inverse method

Matrix inverse method is a case where the writing of the differential equations in matrix form enables one to obtain the response of the system to forced vibration for damped multi degree of freedom system.

Assuming harmonic solution of the form

$$\{X\} = \{A\}\sin\omega t + \{B\}\cos\omega t \qquad (6.2)$$

Substituting equation (4.2) in (4.1) and equating the like terms equations becomes:.

$$\begin{aligned} \left[[K] - \omega^2[M]\{A\}\right] - \omega[C]\{B\} &= \{F\} \\ \omega[C]\{A\} - \left[[K] - \omega^2[M]\{B\}\right] &= \{0\} \end{aligned} \qquad (6.3)$$

Now the above equations can be written as

$$[A]\{X\} = \{F\} \qquad (6.4)$$

Where $[A] = \begin{bmatrix} [[K]-[M]\omega^2]-\omega[C] \\ \omega[C]-[[K]-[M]\omega^2] \end{bmatrix}$ and $\{X\} = \begin{Bmatrix} [A] \\ [B] \end{Bmatrix}$ and $\{F\} = \begin{Bmatrix} \{f\} \\ \{0\} \end{Bmatrix}$

This equation is a matrix equation of order 2n, where n is the degree of freedom of the system. [A] and [B] can be obtained by matrix inversion method

The amplitude is given as

$$X_i = \sqrt{A_i^2 + B_i^2}$$

The c program developed in this thesis simultaneously calculates the desired amplitudes by matrix inverse method. It determines amplitudes with frequency range 0-40Hz. Flow chart of program is given whose

M_1	0	0	0	0	0	0	0	0	0	0	0	0	0	0
0	M_2	0	0	0	0	0	0	0	0	0	0	0	0	0
0	0	M_3	0	0	0	0	0	0	0	0	0	0	0	0
0	0	0	M_4	0	0	0	0	0	0	0	0	0	0	0
0	0	0	0	M_5	0	0	0	0	0	0	0	0	0	0
0	0	0	0	0	M_6	0	0	0	0	0	0	0	0	0
0	0	0	0	0	0	M_7	0	0	0	0	0	0	0	0
0	0	0	0	0	0	0	M_8	0	0	0	0	0	0	0
0	0	0	0	0	0	0	0	M_9	0	0	0	0	0	0
0	0	0	0	0	0	0	0	0	M_{10}	0	0	0	0	0
0	0	0	0	0	0	0	0	0	0	M_{11}	0	0		0
0	0	0	0	0	0	0	0	0	0	0	M_{12}	0	0	0
0	0	0	0	0	0	0	0		0	0	0	M_{13}	0	0
0	0	0	0	0	0	0	0	0	0	0	0	0	M_{14}	0
0	0	0	0	0	0	0	0	0	0	0	0	0	0	M_{15}

MASS MATRIX

Table 6.1 Value of Mass Matrix

3.044	0	0	0	0	0	0	0	0	0	0	0	0	0	0
0	0.207	0	0	0	0	0	0	0	0	0	0	0	0	0
0	0	9.105	0	0	0	0	0	0	0	0	0	0	0	0
0	0	0	2.322	0	0	0	0	0	0	0	0	0	0	0
0	0	0	0	2.322	0	0	0	0	0	0	0	0	0	0
0	0	0	0	0	1.91	0	0	0	0	0	0	0	0	0
0	0	0	0	0	0	1.91	0	0	0	0	0	0	0	0
0	0	0	0	0	0	0	16.55	0	0	0	0	0	0	0
0	0	0	0	0	0	0	0	12.59	0	0	0	0	0	0
0	0	0	0	0	0	0	0	0	7.827	0	0	0	0	0
0	0	0	0	0	0	0	0	0	0	7.827	0	0	0	0
0	0	0	0	0	0	0	0	0	0	0	3.445	0	0	0
0	0	0	0	0	0	0	0	0	0	0	0	3.445	0	0
0	0	0	0	0	0	0	0	0	0	0	0	0	1.998	0
0	0	0	0	0	0	0	0	0	0	0	0	0	0	1.998

Stiffness matrix [K]

K1	-K1	0	0	0	0	0	0	0	0	0	0	0	0	0
-K1	K1+K2	-K2	0	0	0	0	0	0	0	0	0	0	0	0
0	0	K2+K4+K3+K5	-K4	-K5	0	0	-K3	0	0	0	0	0	0	0
0	0	-K4	K4+K6	0	-K6	0	0	0	0	0	0	0	0	0
0	0	-K5	0	K5+K7	0	-K7	0	0	0	0	0	0	0	0
0	0	0	-K6	0	K6	0	0	0	0	0	0	0	0	0
0	0	0	0	-k7	0	K7	0	0	0	0	0	0	0	0
0	0	-K3	0	0	0	0	K3+K8	-K8	0	0	0	0	0	0
0	0	0	0	0	0	0	-K8	K8+K9+K10	-K9	-K10	0	0	0	0
0	0	0	0	0	0	0	0	-K9	K9+K11	0	-K11	0	0	0
0	0	0	0	0	0	0	0	-K10	0	K10+K12	0	-K12	0	0
0	0	0	0	0	0	0	0	0	-K11	0	K11+K13	0	-K13	0
0	0	0	0	0	0	0	0	0	0	-K12	0	K12+K14	0	-K14
0	0	0	0	0	0	0	0	0	0	0	-K13	0	K13+K15	0
0	0	0	0	0	0	0	0	0	0	0	0	-K14	0	K14+K16

s

Damping matrix [C]

C1	-C1	0	0	0	0	0	0	0	0	0	0	0	0	0
-C1	C1+C2	-C2	0	0	0	0	0	0	0	0	0	0	0	0
0	-C2	C2+C4+C3 +C5	-C4	-C5	0	0	-C3	0	0	0	0	0	0	0
0	0	-C4	C4+C6	0	-C6	0	0	0	0	0	0	0	0	0
0	0	-C5	0	C5+C7	0	-C7	0	0	0	0	0	0	0	0
0	0	0	-C6	0	C6	0	0	0	0	0	0	0	0	0
0	0	0	0	-C7	0	C7	0	0	0	0	0	0	0	0
0	0	-C3	0	0	0	0	C3+C8	-C8	0	0	0	0	0	0
0	0	0	0	0	0	0	-C8	C8+C9+C10	-C9	-C10	0	0	0	0
0	0	0	0	0	0	0	0	-C9	C9+C11	0	-C11	0	0	0
0	0	0	0	0	0	0	0	-C10	0	C10+C12	0	-C12	0	0
0	0	0	0	0	0	0	0	0	-C11	0	C11+C13	0	-C13	0
0	0	0	0	0	0	0	0	0	0	-C12	0	C12+C14	0	-C14
0	0	0	0	0	0	0	0	0	0	0	-C13	0	C13+C15	0
0	0	0	0	0	0	0	0	0	0	0	0	-C14	0	C14+C16

Table 6.2 Value of Stiffness matrix (kN/m^2)

680.5	-680.5	0	0	0	0	0	0	0	0	0	0	0	0	0
-680.5	2072.5	-1392	0	0	0	0	0	0	0	0	0	0	0	0
0	-1392	2280.4	-152.1	-152.1	0	0	-584.2	0	0	0	0	0	0	0
0	0	-152.1	250.2	0	-98.1	0	0	0	0	0	0	0	0	0
0	0	152.1	0	250.2	0	-98.1	0	0	0	0	0	0	0	0
0	0	0	-98.1	0	98.1	0	0	0	0	0	0	0	0	0
0	0	0	0	-98.1	0	98.1	0	0	0	0	0	0	0	0
0	0	-584.2	0	0	0	0	1139.3	-555.1	0	0	0	0	0	0
0	0	0	0	0	0	0	-555.1	816.1	-130.5	-130.5	0	0	0	0
0	0	0	0	0	0	0	0	-130.5	199.4	0	-68.9	0	0	0
0	0	0	0	0	0	0	0	-130.5	0	199.4	0	-68.9	0	0
0	0	0	0	0	0	0	0	0	-68.9	0	187.76	0	-118.86	0
0	0	0	0	0	0	0	0	0	0	-68.9	0	187.76	0	-118.86
0	0	0	0	0	0	0	0	0	0	0	-118.86	0	1076.86	0
0	0	0	0	0	0	0	0	0	0	0	0	-118.86	0	1076.86

Table 6.3 Value of Damping Matrix (N-sec/m)

4.8	-4.8	0	0	0	0	0	0	0	0	0	0	0	0	0
-4.8	12.4	-7.6	0	0	0	0	0	0	0	0	0	0	0	0
0	-7.6	20.7	-3.3	-3.3	0	0	-6.5	0	0	0	0	0	0	0
0	0	-3.3	7.98	0	-4.68	0	0	0	0	0	0	0	0	0
0	0	-3.3	0	7.98	0	-4.68	0	0	0	0	0	0	0	0
0	0	0	-4.68	0	4.68	0	0	0	0	0	0	0	0	0
0	0	0	0	-4.68	0	4.68	0	0	0	0	0	0	0	0
0	0	-6.5	0	0	0	0	62.05	-55.55	0	0	0	0	0	0
0	0	0	0	0	0	0	-55.55	1454.97	-699.71	-699.71	0	0	0	0
0	0	0	0	0	0	0	0	-699.71	1734.11	0	-1034.4	0	0	0
0	0	0	0	0	0	0	0	-699.71	0	1734.11	0	-1034.4	0	0
0	0	0	0	0	0	0	0	0	-1034.4	0	1793.47	0	-759.07	0
0	0	0	0	0	0	0	0	0	0	-1034.4	0	1793.47	0	-759.07
0	0	0	0	0	0	0	0	0	0	0	-759.07	0	2475.59	0
0	0	0	0	0	0	0	0	0	0	0	0	-759.07	0	2475.59

Force Matrix for foot and Hand

[F] is the 15x1 column force matrix. All the elements of force matrix are zero except 14^{th} and 15^{th} elements. The 14^{th} and 15^{th} elements are forces on left foot and right foot respectively and in the case of hand all the elements of force matrix are zero except 6^{th} and 7^{th} elements. The 6^{th} and 7^{th} elements are forces on left hand and right hand respectively

Force matrix for Foot	Force matrix for Hand
0	0
0	0
0	0
0	0
0	0
0	100
0	100
0	0
0	0
0	0
0	0
0	0
0	0
100	0
100	0

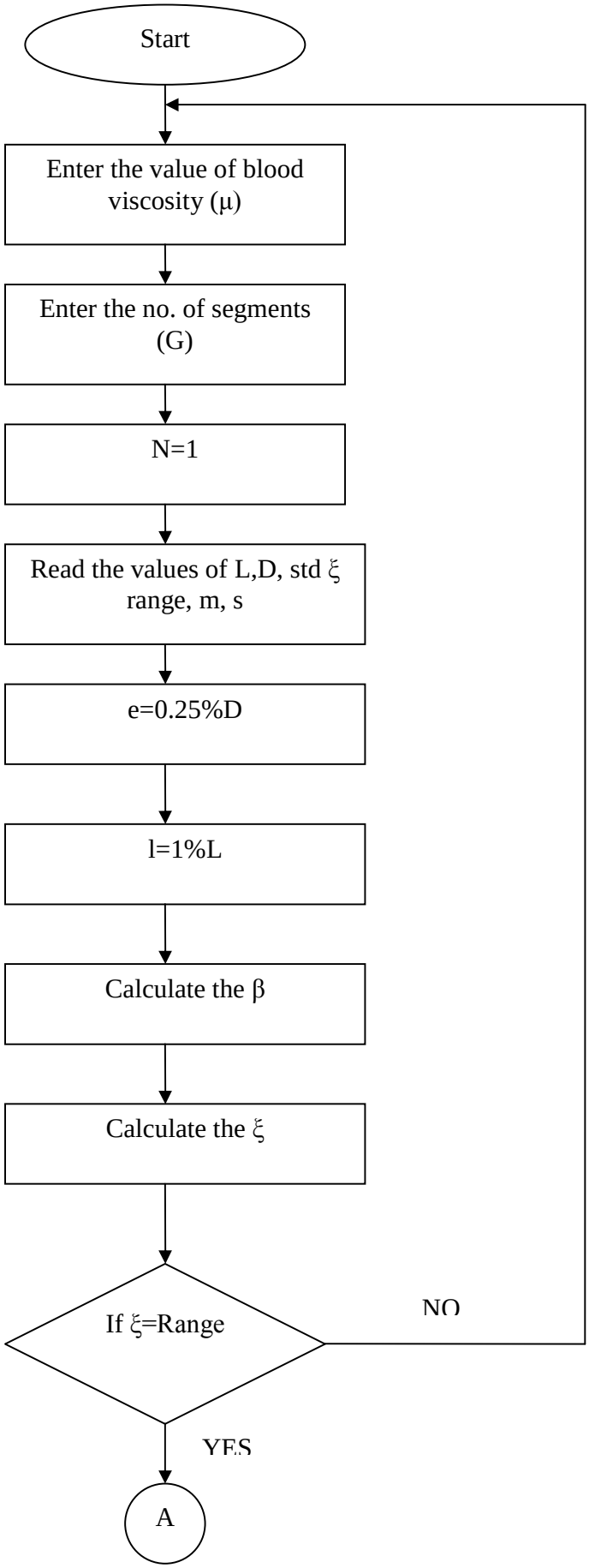
Start
Enter the value of blood viscosity (μ)
Enter the no. of segments (G)
N=1
Read the values of L,D, std ξ range, m, s
e=0.25%D
l=1%L
Calculate the β
Calculate the ξ
If ξ=Range
NO
YES
A

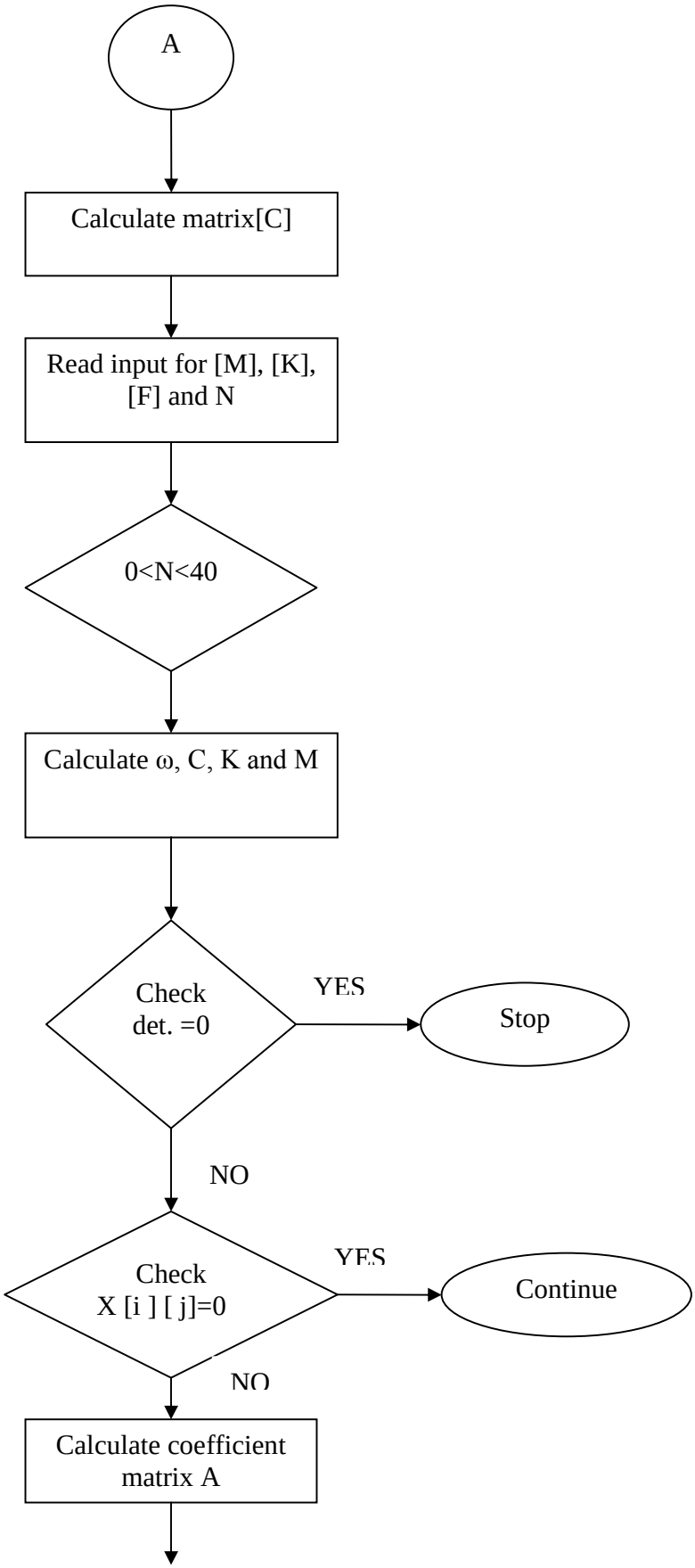
A
Calculate matrix[C]
Read input for [M], [K], [F] and N
0<N<40
Calculate ω, C, K and M
Check det. =0
YES
Stop
NO
Check X [i] [j]=0
YES
Continue
NO
Calculate coefficient matrix A

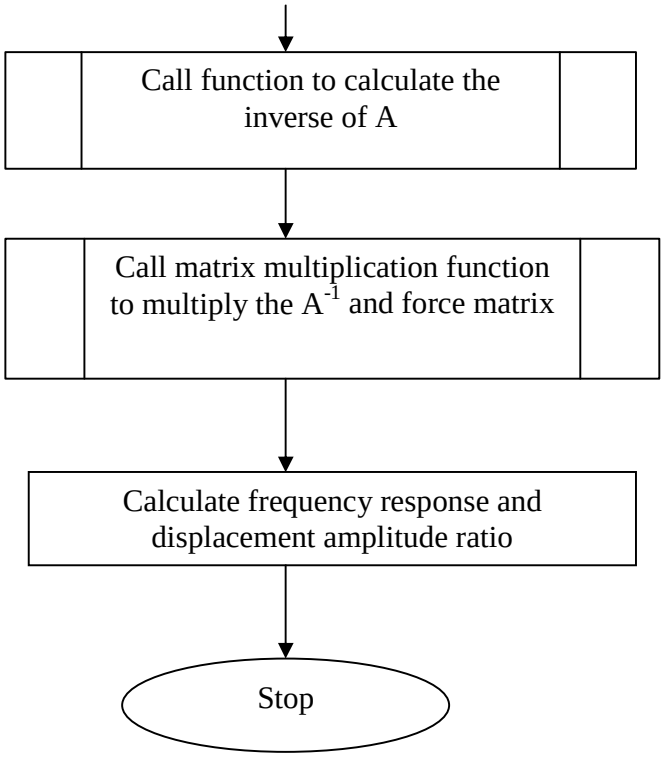

Fig. 6.1 Flow chart of main program

Chapter-7

RESULTS AND DISCUSSION

For analyzing the vibration characteristics of a machine and structures, one of the important steps is to model the system by schematic arrangement of masses, elastic elements and damping elements. A real human subject cannot be broken up as individual components like in mechanical structures. In general there is no uniform human body available in real life applications due to variation in size, age, sex and weight etc. Similar to the vibratory modeling of any machine or structure the vibratory model of human body has to be initially framed as a basic spring-mass system. Further development in the vibratory model of human body can then be made by incorporating necessary damping values of viscous fluids of human body.

In the present analysis an initial effort has been made to analytically evaluate the damping coefficients of the individual segments by considering the viscosity of blood and synovial fluid (plasma) and damping values in the proposed model have been obtained to analyze the model frequency response.

7.1 NATURAL FREQUENCY

The natural frequencies as obtained by generalized Jacobi method [30] are given in Table 7.1, where the natural frequency of zero pertains to the rigid body mode of semi-definite system. The other frequencies are below 200 Hz and this signifies the importance of the presence of lower frequencies in comfort studies and response of human beings subjected to different excitation.

Table 7.1: Computed natural frequency (Hz)

f1	f2	f3	f4	f5	f6	f7	f8	f9	f10	f11	f12	f13	f14	f15
13.82	14.35	23.92	25.22	28.77	29.53	40.29	53.32	59.00	58.65	79.25	165.32	165.6	207.9	207.6

7.2: FREQUENCY RESPONSE OF THE SYSTEM

The two force situations that have been considered are:

1) 100N force applied at foot (for e.g. human standing at vibratory platform)M14 and M15.
2) 100N force applied at hand (for e.g. in grinding operation) M6 and M7.

Corresponding to each of the above, frequency responses have been obtained in terms of displacement amplitude vs. excitation frequency.

7.3 FREQUENCY RESPONSE OF DIFFERENT BODY SEGMENTS DUE TO CONSTANT FORCE (100N) EXCITATION AT M14 AND M15 (FOOT)

The absolute amplitudes for the different segments of the system masses for a constant force of 100N acting on mass M14 and M15 have been evaluated with the help of eq.6.4. The excitation frequency is varied from 0Hz to 40Hz. Frequency response curves are plotted (Fig 7.1-7.10) for different body segments with amplitudes against excitation frequencies. Garg and Ross [6] performed experiments on young males of 20-25 years and gave the response plots. They reported in their work that the resonance peaks occur at 2, 6 and 20 Hz. The 2Hz resonance peak is due to the mass and stiffness of internal organs. The mass of whole body on the stiffness of the legs results in a response near 20Hz. In the present work excitation frequency range takes upto0-40Hz only because at higher excitation frequency, effect of excitation is negligible.

7.4 FREQUENCY RESPONSE OF DIFFERENT BODY SEGMENTS DUE TO CONSTANT FORCE (100N) EXCITATION AT M6 AND M7 (HAND)

Hand arm vibration is the second area where transmission of vibration into the human body is concerned. Vibration levels encountered in many commonly used power tools are sufficiently high to cause damage when operated for durations common in industry. Typical of these power tools are chipping hammers, power grinders, hammer drills and chain saws which are found in widespread use in the mining, construction and manufacturing industries.

Vibration may be transmitted to the body from a vibrating tool or hand held work piece via one or both arms simultaneously. These effects and their cause are currently being extensively investigated both by medical and engineering researchers.

In this theoretical model a force of 100N is applied on mass M6 and M7. The amplitudes of vibration for different segments of the system have been evaluated with the help of eq 6.4. The excitation frequency is varied from 0 Hz to 40 Hz. Response curves are given in Fig. 7.1-7.10.

The resonant frequencies found in Table 7.2 &7.3 match with the resonant frequencies reported by Garg and Ross [6]. The first peak is same for both the situations, force at foot (M14 and M15) and force at hands (M6 and M7), but the vibration amplitudes are always not higher in the second case at all the frequencies, and depend on the location of the mass segments.

The amplitudes are changed considerably by individual differences in the body, the posture of the body, or by the state of the knee or ankle joints of standing subjects. The first resonant frequency remains constant at 2 Hz. Above 2 Hz vibration displacements amplitude of the body are decreasing continuously with increasing frequencies.

Frequency response of different body segments

The frequency response curves for different body segments M1, M2, M3, M4/M5, M6/M7, M8, M9, M10/M11, M12/M13 and M14/M15 are plotted for a force of 100N at M14 & M15 and at M6 & M7. From the graphs it is seen that first peak for all the segments occurs at 2 Hz. Some of the resonance peaks from response plots for different body segments are shown in Table 7.2 &7.3. The given set of resonance frequencies matches with the resonance frequencies reported by Garg and Ross [6]. This proves the correctness of method and computer program developed in this work.

The input/output properties of head–neck system have not been studied over its full dynamic range. The center of gravity can be considered in front of the neck joint, which permits forward- backward motion. This situation results in forward backward rotation of the head instead of pure vertical motion [24]. This requires further investigation.

In this work, the graphs are plotted when force is applied at M14/M15 (foot) and at M6/M7 (hand). The graphs are superimposed for all body segments for comparison. These are discussed one by one.

Table 7.2: Force applied at foot M14 and M15

(Amplitude in mm*100)

F(Hz)	X1	X2	X3	X4=X5	X6=X7	X8	X9	X10=X11	X12=X13	X14=X15
0	0.61	0.61	0.61	0.61	0.61	0.61	0.61	0.62	0.62	0.63
2	**1.52**	**1.42**	**1.43**	**1.53**	**1.58**	**1.26**	**1.13**	**1.42**	**0.87**	**0.67**
4	0.75	0.71	0.71	0.87	1.45	0.42	0.07	0.03	0.25	0.57
6	0.51	0.4	0.38	0.72	1.01	0.14	**0.48**	**0.54**	**0.57**	**0.59**
8	0.15	0.12	0.12	0.43	**1.26**	**0.54**	0.42	0.43	0.42	0.56
10	**0.70**	**0.63**	**0.58**	0.07	1.08	0.38	0.29	0.38	**0.48**	0.55
12	0.61	0.53	0.48	0.27	0.57	0.23	**0.35**	0.33	0.33	0.47
14	0.45	0.36	0.32	**0.31**	0.32	**0.51**	0.23	0.31	**0.45**	0.41
16	0.09	0.07	0.06	0.08	0.04	0.19	**0.26**	0.29	0.31	0.36
18	0.03	0.02	0.02	0.05	0.03	0.07	0.2	0.21	0.22	0.34
20	**0.06**	**0.05**	**0.04**	0.03	0.02	0.04	0.18	0.18	0.2	0.31
22	0.03	0.02	0.01	0.02	0.02	0.03	0.17	0.16	0.18	0.29
24	0.01	0.01	0.01	0.02	0.01	0.03	0.15	0.12	0.17	0.27
26	0.01	0.01	0.01	0.01	0.01	0.02	0.09	0.09	0.16	0.25
28	**0.02**	0.01	**0.03**	0.004	0.008	0.02	0.08	0.08	0.15	0.24
30	0.01	0.01	0.008	0.003	0.008	0.01	0.07	0.07	0.13	0.23
32	0.01	0.01	0.008	0.003	0.007	0.007	0.06	0.05	0.09	0.23
34	0.01	0.01	0.007	0.002	0.006	0.006	0.05	0.05	0.09	0.22
36	0.01	0.01	0.006	0.002	0.005	0.005	0.04	0.04	0.08	0.21
38	0.01	0.01	0.005	0.001	0.005	0.005	0.03	0.03	0.07	0.20
40	0.01	0.01	0.005	0.001	0.001	0.001	0.02	0.02	0.07	0.19

Table 7.3: Force applied at hand M6 and M7

(Amplitude in mm*10)

F(Hz)	X1	X2	X3	X4=X5	X6=X7	X8	X9	X10=X11	X12=X13	X14=X15
0	2	2	2	2	2	2	2	2	0.615	0.62
2	**4.12**	**4**	**4.1**	**4.55**	**5.35**	**3.25**	**2.58**	**2.25**	**1.32**	**1.58**
4	1.65	1.63	1.6	1.58	1.45	1.62	1.3	1.35	0.758	1.08
6	1.1	1	1	1.15	2.05	1.35	1.22	1.18	0.647	1.21
8	1.25	**1.32**	**1.28**	**1.35**	**2.24**	1.2	1.05	1.05	0.61	**1.3**
10	**1.32**	1.2	0.92	0.98	1.95	0.87	0.759	0.85	0.5	1.23
12	0.68	0.6	0.45	0.52	1.2	0.62	0.425	0.42	0.325	0.61
14	0.55	0.5	0.324	0.28	0.85	0.35	0.225	0.26	0.1958	0.35
16	0.38	0.42	0.22	0.32	0.45	0.112	0.025	0.032	0.035	0.0425
18	0.45	0.39	0.28	0.62	0.28	0.098	0.02	0.026	0.023	0.032
20	**0.75**	**0.65**	**0.34**	**1.2**	**0.75**	0.045	0.015	0.02	0.02	0.026
22	0.15	0.092	0.01	0.32	0.32	0.032	0.012	0.018	0.018	0.02
24	0.092	0.042	0.002	0.12	0.22	0.024	0.01	0.013	0.013	0.017
26	0.07	0.018	0.002	0.115	0.198	0.02	0.01	0.01	0.01	0.012
28	**0.18**	0.015	**0.048**	0.01	0.185	0.018	0.009	0.01	0.01	0.01
30	0.046	0.013	0.003	**0.085**	0.172	0.01	0.0084	0.0084	0.0084	0.0084
32	0.013	0.0132	0.002	0.002	0.164	0.006	0.006	0.006	0.006	0.006
34	0.0132	0.012	0.003	0.003	0.155	0.002	0.002	0.002	0.002	0.002
36	0.012	0.012	0.001	0.001	0.143	0.003	0.003	0.003	0.003	0.003
38	0.012	0.012	0.001	0.001	0.132	0.001	0.001	0.001	0.001	0.001
40	0.012	0.01	0.001	0.001	0.112	0.001	0.001	0.001	0.001	0.001

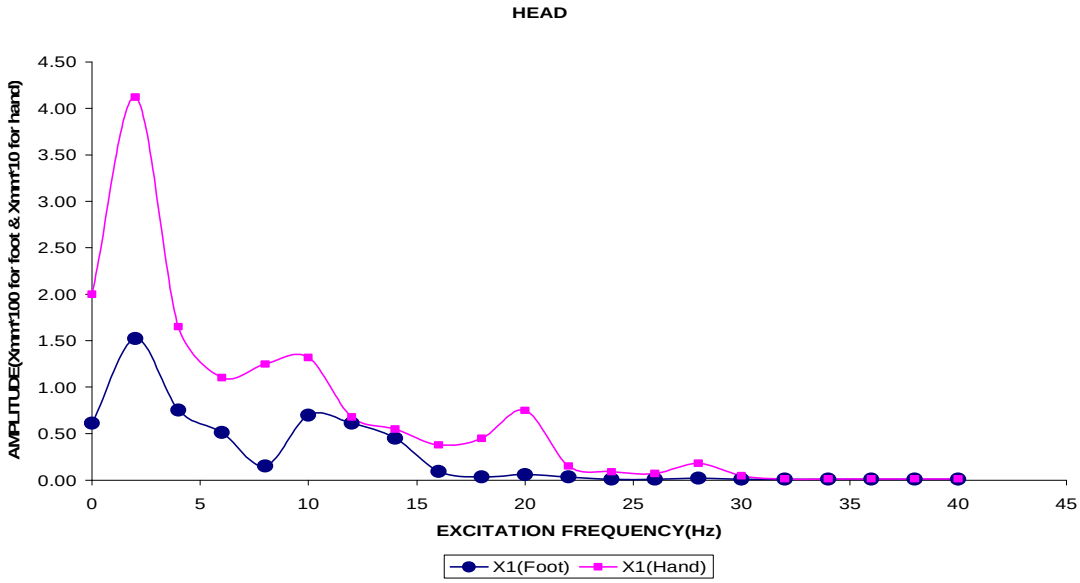

Fig 7.1. FREQUENCY RESPONSE OF M1(HEAD) FOR FORCE=100N ON M14/M15 (FOOT) AND M6/M7 (HAND)

For a 100N force applied at M14/M15 (foot), it is seen that the response of head at the fundamental peak occurs at excitation frequency of 2Hz, and other peaks occur at 10Hz, 20 Hz and 28Hz. The four amplitude responses of head are $1.52*10^{-2}$, $0.70*10^{-2}$, $0.06*10^{-2}$ and $0.02*10^{-2}$ mm, respectively. The effect on head of excitation frequency greater 30Hz is negligible. It can be noted that the low frequency response travels from foot to head and head does not respond to the high frequency excitations.

When a 100N force is applied at M6/M7 (hand), it is seen the response of head at the fundamental peak occurs once again at excitation frequency of 2Hz, and other peaks occur at 10Hz, 20 Hz and 28Hz. The four amplitude responses of head are $4.12*10^{-1}$, $1.32*10^{-1}$, $0.75*10^{-1}$ and $0.18*10^{-1}$ mm, respectively. The effect on head of excitation frequency becomes negligible after 30Hz. It can be seen that the low frequency response travels from hand to head and head does not respond to the high frequency excitation.

The effect of vibration is dependent on the proximity of head with the excitation points at hand and foot as expected and it is clearly seen in the graph. At 12Hz excitation frequency, amplitude of head is nearly same in both cases. At higher excitation frequency, effect of excitation is negligible at head, in both the cases. As excitation frequency increases the response amplitude at head gradually decreases, beyond higher excitation frequency, in both the cases, but some isolated peaks are observed after 12Hz for hand excitation.

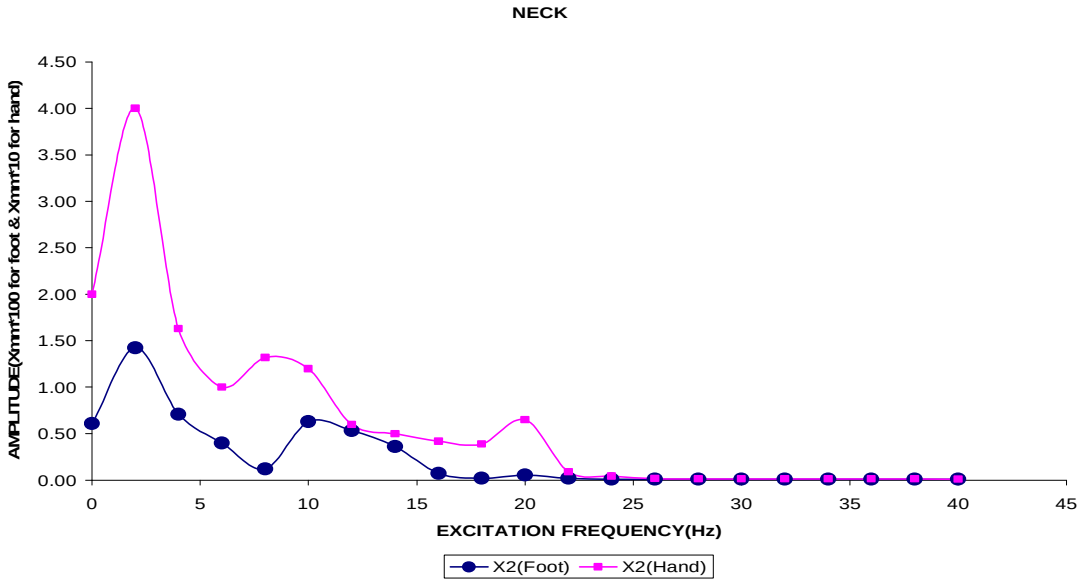

Fig 7.2. FREQUENCY RESPONSE OF M2(NECK) FOR FORCE=100N ON M14/M15 (FOOT) AND M6/M7 (HAND)

For a 100N force applied at M14/M15 (foot), it is seen that the response of neck at the fundamental peak occurs at excitation frequency of 2Hz, and other peaks occur at 10Hz and 20Hz. The three amplitude responses of neck are $1.42*10^{-2}$, $0.63*10^{-2}$ and $0.052*10^{-2}$ mm, respectively. The effect on neck of excitation frequency greater 28Hz is negligible. It can be seen that the low frequency response travels from foot to neck and neck does not respond to the high frequency excitation.

When a 100N force is applied at M6/M7 (hand), it is seen the response of neck at the fundamental peak occurs once again at excitation frequency of 2Hz, and other peaks occur at 8 Hz and 20Hz. The three amplitude responses of neck are 4.00, $*10^{-1}$ $1.32*10^{-1}$ and $0.65*10^{-1}$ mm, respectively. The effect on neck of excitation frequency becomes negligible after 28Hz. It can be seen that the low frequency response travels from hand to neck and neck does not respond to the high frequency excitation.

The effect of vibration is dependent on the proximity of neck with the excitation points at hand and foot as expected and it is clearly seen in the graph. At 12Hz excitation frequency, amplitude of neck is nearly same in both cases. At higher excitation frequency, effect of excitation is negligible at neck, in both the cases. As excitation frequency increases the response amplitude at neck gradually decreases, beyond large excitation frequency, in both the situations, but some isolated peaks are observed after 12Hz, for hand excitation.

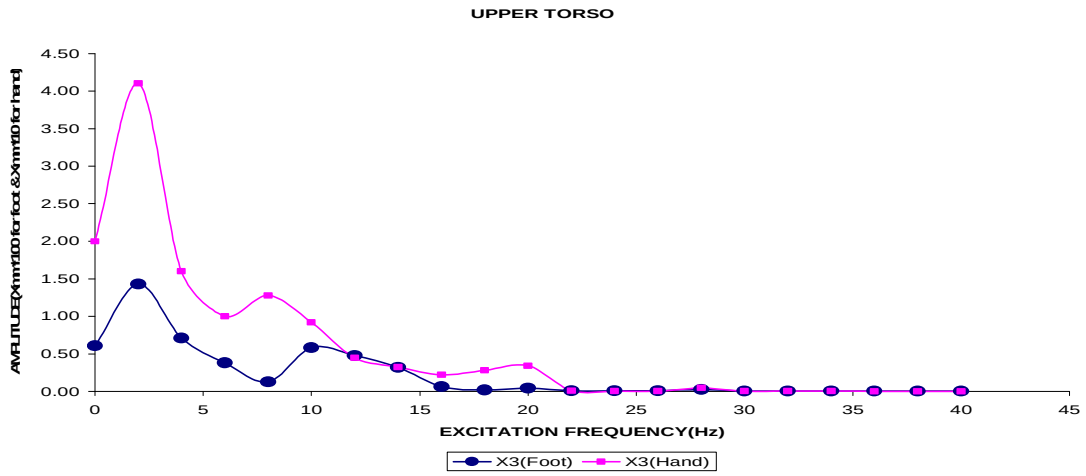

Fig 7.3. FREQUENCY RESPONSE OF M3(UPPER TORSO) FOR FORCE=100N ON M14/M15 (FOOT) AND M6/M7 (HAND)

For a 100N force applied at M14/M15 (foot), it is seen that the response of upper torso at the fundamental peak occurs at excitation frequency of 2Hz, and other peaks occur at 10Hz, 20 Hz and 28Hz. The four amplitude responses of upper torso are $1.43*10^{-2}$, $0.583*10^{-2}$, $0.042*10^{-2}$ and $0.03*10^{-2}$ mm, respectively. The effect on upper torso of excitation frequency greater 30Hz is negligible. It can be seen that the low frequency response travels from foot to upper torso and the upper torso does not respond to the high frequency excitation.

When a 100N force is applied at M6/M7 (hand), it is seen that the response of upper torso at the fundamental peak occurs at excitation frequency of 2Hz, and other peaks occur at 8Hz, 20Hz and 28Hz. The four amplitude responses of upper torso are $4.10*10^{-1}$, $1.28*10^{-1}$, $0.34*10^{-1}$ and $0.048*10^{-1}$ mm, respectively. The effect on upper torso of excitation frequency becomes negligible after 30Hz. It can be seen that the low frequency response travels from hand to upper torso and the upper torso does not respond to the higher frequency excitation.

The effect of vibration is dependent on the proximity of upper torso with the excitation points at hand and foot as expected and it is clearly seen in the graph. At 12Hz and 14Hz excitation frequency, amplitude of upper torso is nearly same in both cases. At higher excitation frequency, effect of excitation is negligible at upper torso, in both the cases. As excitation frequency increases the response amplitude at upper torso gradually decreases, beyond large excitation, in both the situations, but some isolated peaks are noted after 12Hz, for hand excitation.

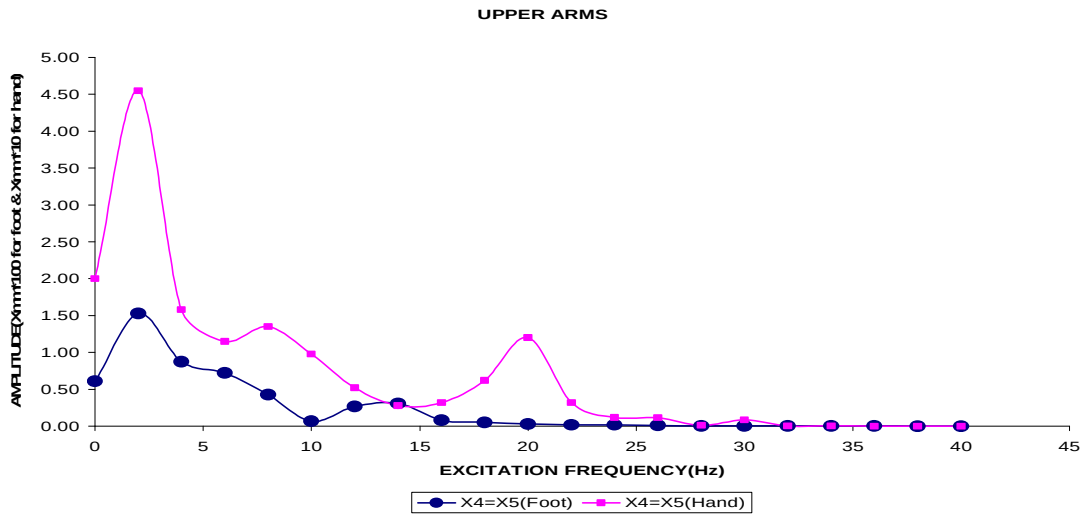

Fig 7.4. FREQUENCY RESPONSE OF M4=M5(UPPER ARMS) FOR FORCE=100N ON M14/M15 (FOOT) AND M6/M7 (HAND)

For a 100N force applied at M14/M15 (foot), it is seen that the response of upper arms at the fundamental peak occurs at excitation frequency of 2Hz, and other peaks occur at 14Hz. The two amplitude responses of upper arms are $1.53*10^{-2}$ and $0.31*10^{-2}$ mm, respectively. The effect on upper arms of excitation frequency greater 22Hz is negligible. It can be observed that the low frequency response travels from foot to upper arms and the upper arms do not respond to the high frequency excitation.

When a 100N force is applied at M6/M7 (hand), it is seen the response of upper arms at the fundamental peak occurs once again at excitation frequency of 2Hz, and other peaks occur at 8Hz, 20Hz and 30Hz. The four amplitude responses of upper arms are $4.55*10^{-1}$, $1.35*10^{-1}$, $1.20*10^{-1}$ and $0.085*10^{-2}$ mm, respectively. The effect on upper arms of excitation frequency becomes negligible after 30Hz. It can be observed that the low frequency response travels from hand to upper arms and the upper arms do not respond to the high frequency excitation.

The effect of vibration is dependent on the proximity of upper arms with the excitation points at hand and foot as expected and it is clearly seen in the graph. At 14Hz excitation frequency, amplitude of upper arms is nearly same in both cases. At higher excitation frequency effect of excitation is negligible at upper arms, in both the cases. As excitation frequency increases the response amplitude at upper arms gradually decreases, beyond large frequency, in both the situations, but some isolated peaks are observed after 14Hz, for hand excitation.

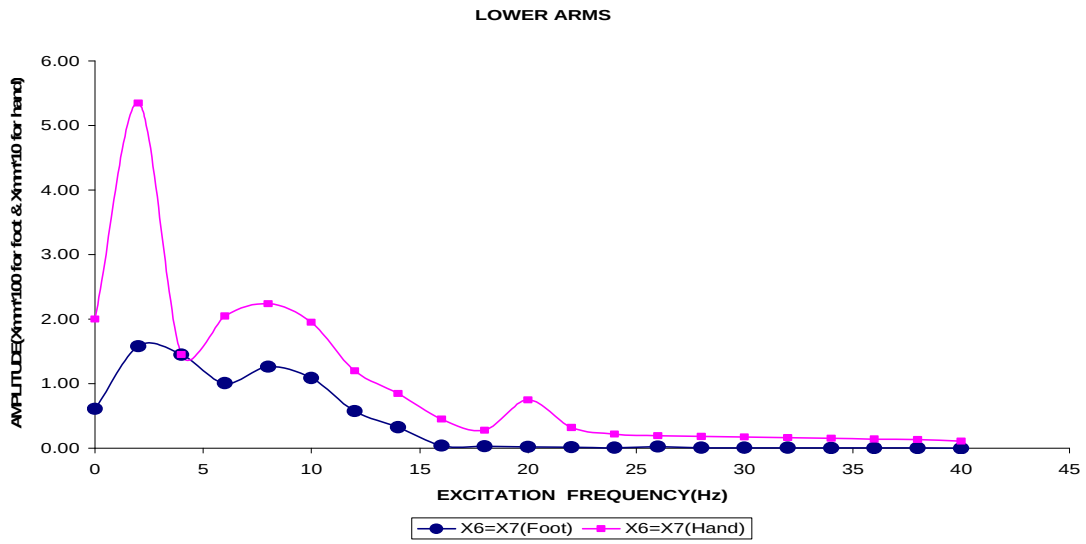

Fig 7.5. FREQUENCY RESPONSE OF M6=M7(LOWER ARM) FOR FORCE=100N ON M14/M15 (FOOT) AND M6/M7 (HAND)

For a 100N force applied at M14/M15 (foot), it is seen that the response of lower arms at the fundamental peak occurs at excitation frequency of 2Hz, and other peak occurs at 8Hz. The two amplitude responses of lower arms are $1.58*10^{-2}$ and $1.26*10^{-2}$ mm, respectively. The effect on lower arms of excitation frequency greater 20Hz is negligible. It can be seen that the low frequency response travels from foot to lower arms and the lower arms do not respond to the high frequency excitation.

When a 100N force is applied at M6/M7 (hand), it is seen the response of lower arms at the fundamental peak occurs at excitation frequency of 2Hz, and other peaks occur at 8Hz and 20Hz. The three amplitude responses of lower arms are $5.35*10^{-1}$, $2.24*10^{-1}$ and $0.75*10^{-1}$ mm, respectively. The effect on lower arms of excitation frequency decreases after 24Hz. It can be seen that the low frequency response travels from hand to lower arms and the lower arms response decrease to the high frequency excitation.

The effect of vibration is dependent on the proximity of lower arms with the excitation points at hand and foot as expected and it is clearly seen in the graph. At 4Hz excitation frequency, amplitude of lower arms is nearly same in both cases. At higher excitation frequency, effect of excitation is negligible (in case of foot) and decrease (in case of hand) on lower arms. As excitation frequency increases the response amplitude at lower arms gradually decreases, beyond large frequency, in both the situations, but some isolated peaks are observed after 14Hz, for hand excitation.

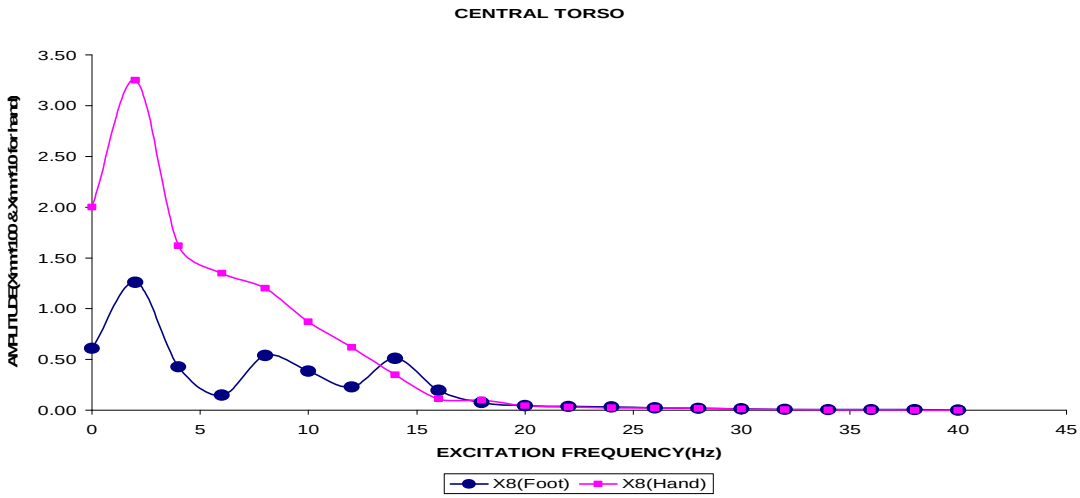

Fig 7.6. FREQUENCY RESPONSE OF M8(CENTRAL TORSO) FOR FORCE=100N ON M14/M15 (FOOT) AND M6/M7 (HAND)

For a 100N force applied at M14/M15 (foot), it is seen that the response of central torso at the fundamental peak occurs at excitation frequency of 2Hz, and other peaks occur at 8Hz and 14Hz. The three amplitude responses of central torso are $1.26*10^{-2}$, $0.54*10^{-2}$ and $0.51*10^{-2}$ mm, respectively. Central torso is directly connected to foot so the some isolated peaks are observed. The effect on central torso of excitation frequency greater 24Hz is negligible. It can be noted that the low frequency response travels from foot to central torso and the central torso does not respond to the high frequency excitation.

When a 100N force is applied at M6/M7 (hand), it is seen that the response of central torso at the fundamental peak occurs at excitation frequency of 2Hz, and no peaks occur after 2Hz. The one amplitude response of central torso is $3.25*10^{-1}$mm, respectively. The effect on central torso of excitation frequency becomes negligible after 24Hz. It can be noted that the low frequency response travels from hand to central torso and the central torso does not respond to the high frequency excitation.

The effect of vibration is dependent on the proximity of central torso with excitation points at hand and foot as expected and it is clearly seen in the graph. At 18Hz and 20Hz excitation frequency, amplitude of central torso is nearly same in both cases. At higher excitation frequency effect of excitation is negligible at central torso, in both the cases. As excitation frequency increases the response amplitude at central torso gradually decreases, beyond large frequency, in both the situations, but some isolated peaks are observed after 12Hz, for foot excitation.

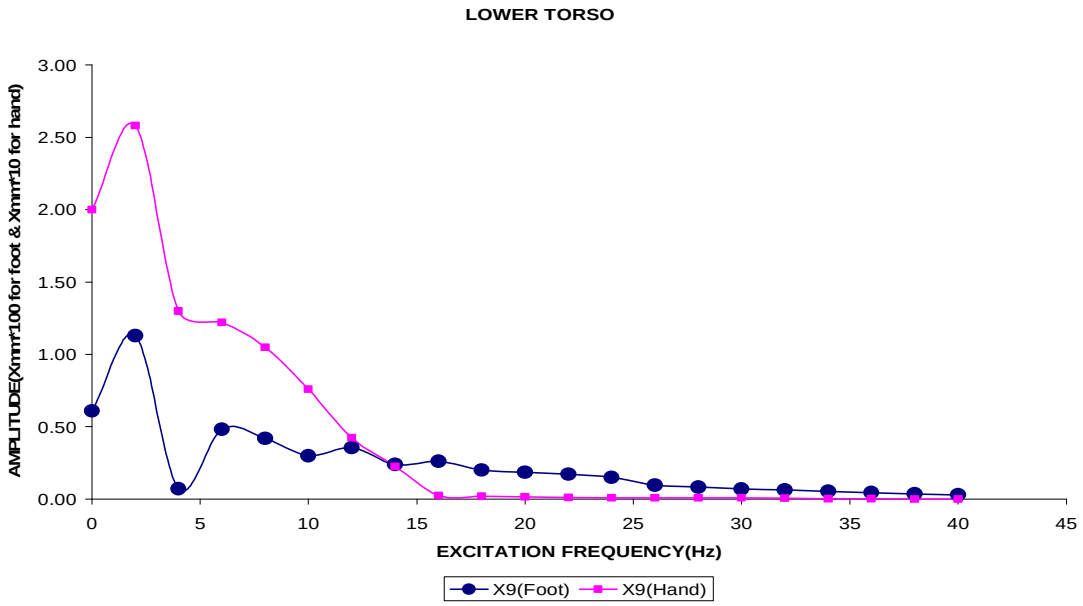

Fig 7.7. FREQUENCY RESPONSE OF M9(LOWER TORSO) FOR FORCE=100N ON M14/M15 (FOOT) AND M6/M7 (HAND)

For a 100N force applied at M14/M15 (foot), it is seen that the response of lower torso at the fundamental peak occurs at excitation frequency of 2Hz, and other peaks occur at 6Hz, 12Hz and 16Hz. The four amplitude responses of lower torso are $1.13*10^{-2}$, $0.48*10^{-2}$, $0.35*10^{-2}$ and $0.26*10^{-2}$ mm, respectively. The effect of excitation frequency at lower torso gradually decreases after 18Hz. It can be observed that the low frequency response travels from foot to lower torso and the lower torso response decrease to the high frequency excitation.

When a 100N force is applied at M6/M7 (hand), it is seen that the response of lower torso at the fundamental peak occurs at excitation frequency of 2Hz, and no peaks occur after 2Hz. The one amplitude response of lower torso is $2.58*10^{-1}$ mm, respectively. The effect on lower torso of excitation frequency greater 16Hz is negligible. It can be noted that the low frequency response travels from hand to lower torso and the lower torso does not responded to the high frequency excitation.

The effect of vibration is dependent on the proximity of lower torso with the excitation points at hand and foot as expected and it is clearly seen in the graph. At 14Hz excitation frequency, amplitude of lower torso is nearly same in both the cases. Beyond cross over frequency (C.O.F) response of lower torso (which is attached to feet) is visible, while it is negligible for excitation at hand.

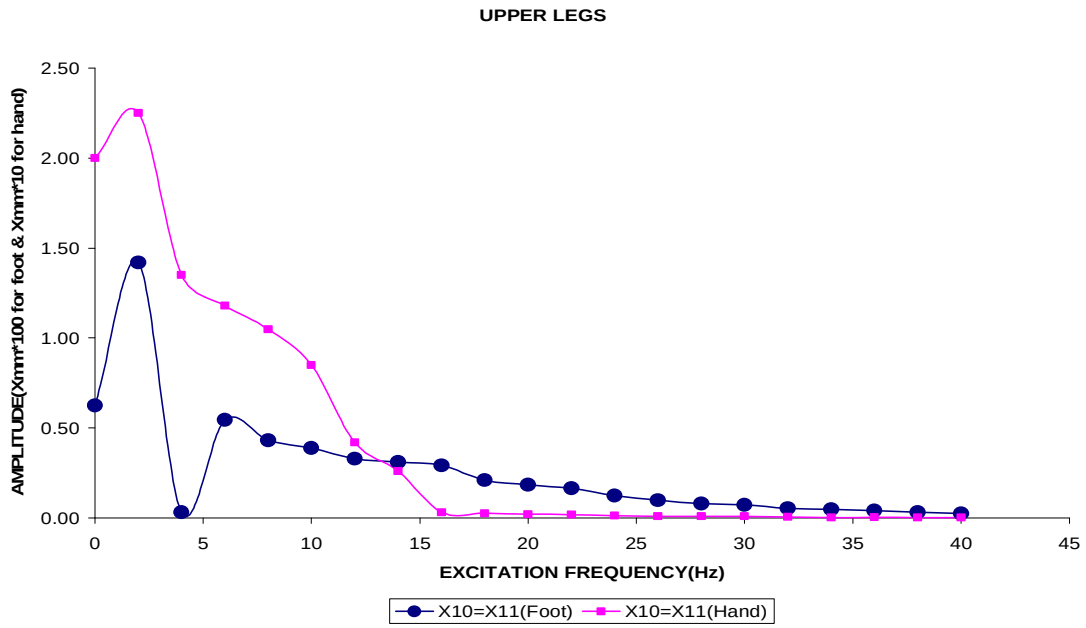

Fig 7.8. FREQUENCY RESPONSE OF M10=M11(UPPER LEGS) FOR FORCE=100N ON M14/M15 (FOOT) AND M6/M7 (HAND)

For a 100N force applied at M14/M15 (foot), it is seen that the response of upper legs at the fundamental peak occurs at excitation frequency of 2Hz, and other peak occurs at 6Hz, after 6Hz no peaks occur. The two amplitude responses of upper legs are $1.42*10^{-2}$ and $0.54*10^{-2}$ mm, respectively. The effect of excitation frequency at upper legs gradually decreases after 8Hz. It can be seen that the low frequency response travels from feet to upper legs and the upper legs response decrease to the high frequency excitation. After 14Hz no prominent peaks occur.

When a 100N force is applied at M6/M7 (hand), it is seen that the response of upper legs at the fundamental peak occurs at excitation frequency of 2Hz, and no peaks occur after 2Hz. The one amplitude response of upper leg is $2.25*10^{-1}$ mm, respectively. The effect on upper legs of excitation frequency becomes negligible after 16Hz. It can be seen that the low frequency response travels from hand to upper legs and the upper legs does not response to the high frequency excitation.

The effect of vibration is dependent on the proximity of upper legs with excitation points at hand and foot as expected and it is clearly seen in the graph. At 14Hz excitation frequency, amplitude of upper legs is nearly same in both cases. Beyond cross over frequency (C.O.F) response of upper legs (which is attached to feet) is visible, while it is negligible for excitation at hand.

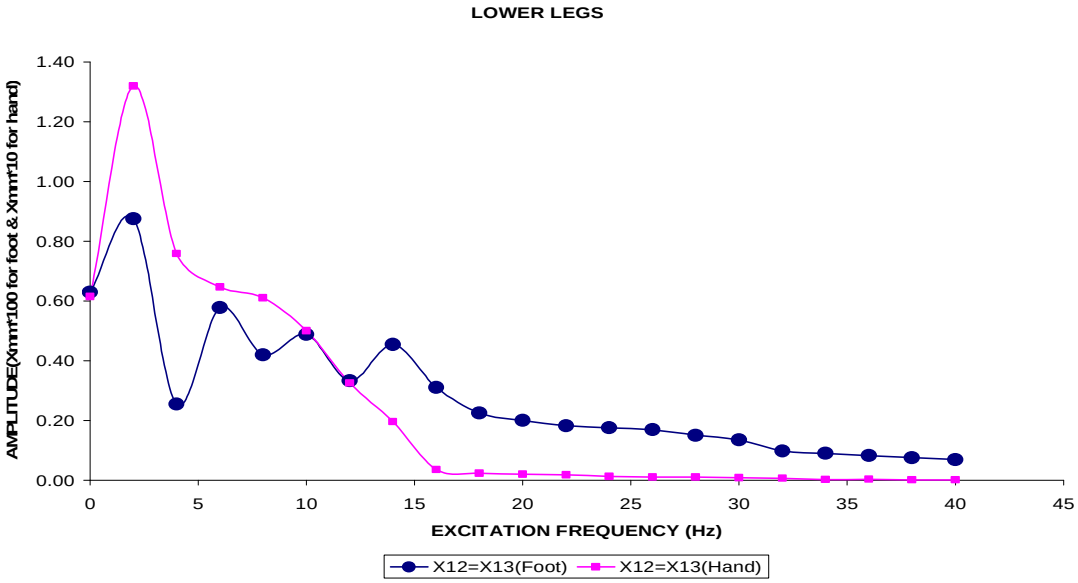

Fig 7.9. FREQUENCY RESPONSE OF M10=M11(LOWER LEGS) FOR FORCE=100N ON M14/M15 (FOOT) AND M6/M7 (HAND)

For a 100N force applied at M14/M15 (foot), it is seen that the response of lower legs at the fundamental peak occurs at excitation frequency of 2Hz, and other peaks occur at 6Hz, 10Hz and 14Hz, after 14Hz no peaks occur. The four amplitudes response of lower legs are $0.87*10^{-2}$, $0.57*10^{-2}$, $0.48*10^{-2}$ and $0.45*10^{-2}$ mm, respectively. The effect on lower legs of excitation frequency gradually decreases after 16Hz. It can be observed that the low frequency response travels from feet to upper legs and the upper legs response continuous decrease to the high frequency excitation. After 14Hz no prominent peaks occur.

When a 100N force is applied at M6/M7 (hand), it is seen that the response of lower legs at the fundamental peak occurs at excitation frequency of 2Hz, and no peaks occur after 2Hz. The one amplitude found in response of lower leg is $1.32*10^{-1}$ mm, respectively. The effect on lower legs of excitation frequency becomes negligible after 16Hz. It can be observed that the low frequency response travels from hand to lower legs and the lower legs does not response to the high frequency excitation.

The effect of vibration is dependent on the proximity of lower legs with excitation points at hand and foot as expected and it is clearly seen in the graph. At 10Hz and 12Hz excitation frequency, amplitude of lower legs is nearly same in both cases. Beyond cross over frequency (C.O.F) response of lower legs (which is attached to feet) is visible, while it is negligible for excitation at hand.

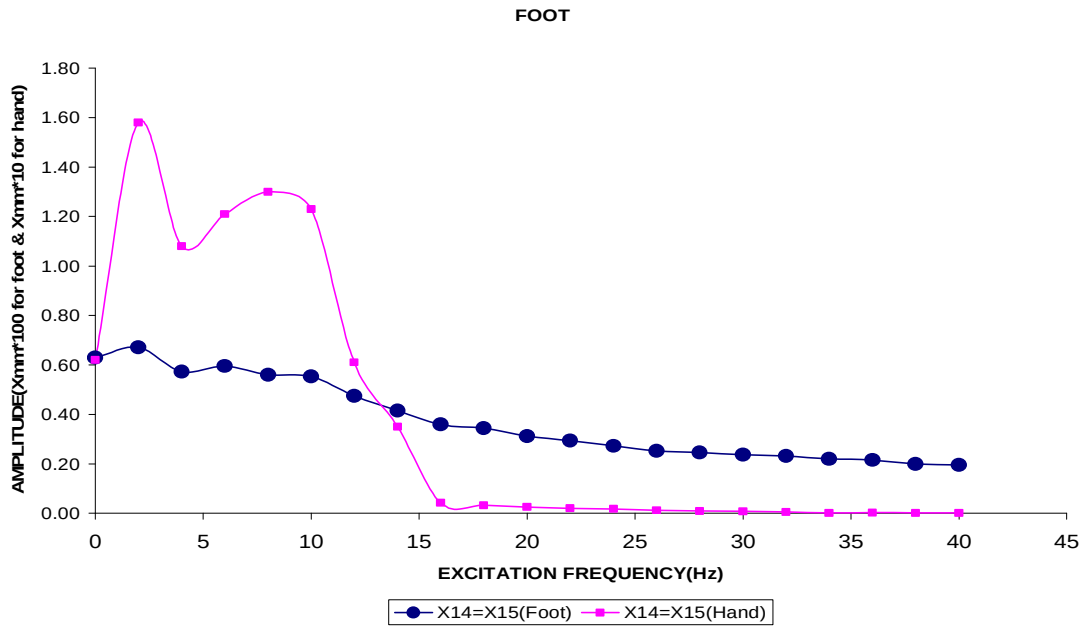

Fig 7.10. FREQUENCY RESPONSE OF M14=M15(FEET) FOR FORCE=100N ON M14/M15 (FOOT) AND M6/M7 (HAND)

For a 100N force applied at M14/M15 (foot), it is seen that the response of foot at the fundamental peak occurs at excitation frequency of 2Hz, and other peaks occur at 6Hz and 10Hz, after 12Hz no peaks occur. The three amplitude responses of foot are $0.67*10^{-2}$, $0.59*10^{-2}$ and $0.55*10^{-2}$ mm, respectively. The effect on feet of excitation frequency gradually decreases after 14Hz, when force is acting on it with increase in excitation frequency. It can be observed that the low frequency response travels from feet to upper legs and the upper legs response continuous decrease to the high frequency excitation. After 14Hz no prominent peaks occur.

When a 100N force is applied at M6/M7 (hand), it is seen that the response of foot at the fundamental peak occurs at excitation frequency of 2Hz, other peak occurs at 8Hz and no peaks occur after 12Hz. The two amplitude responses of foot are $1.58*10^{-1}$ and $1.30*10^{-1}$ mm, respectively. The effect on foot of excitation frequency becomes negligible after 16Hz. It can be observed that the low frequency response travels from hand to feet and the feet does not response to the high frequency excitation.

The effect of vibration is dependent on the proximity of foot with excitation points at hand and foot as expected and it is clearly seen in the graph. At 14Hz excitation frequency, amplitude of foot is nearly same in both cases. Beyond cross over frequency (C.O.F)

response of foot (which is attached to feet) is visible, while it is negligible for excitation at hand.

The combination of soft tissue and bone in the structure of the body together with the bodies geometric dimensions result in a system which exhibits different types of response depending on the frequency range. At the low frequencies the body can be described as a lumped parameter system, resonance occurred due to the interaction of tissue masses with purely elastic structures [24].

This concluded that the human body segments are more prone to low frequency excitations only and slow peaks in frequency response. At high frequency the response gradually decreases and beyond certain frequency, it is practically negligible.

7.5 Damping values at fundamental mode

The damping values have been evaluated from the response plots at fundamental modes by the equation, given below

$$2\xi = \frac{\omega_2 - \omega_1}{\omega_n} \qquad (7.1)$$

Where

ξ= Damping ratio

ω_1 and ω_2 =A horizontal line cutting the response curve at 0.707R (Half power points) two points, the corresponding values of abscissa being ω_1 and ω_2.

ω_n = natural frequency

ω_1, ω_2 and ω_n are as shown in Fig

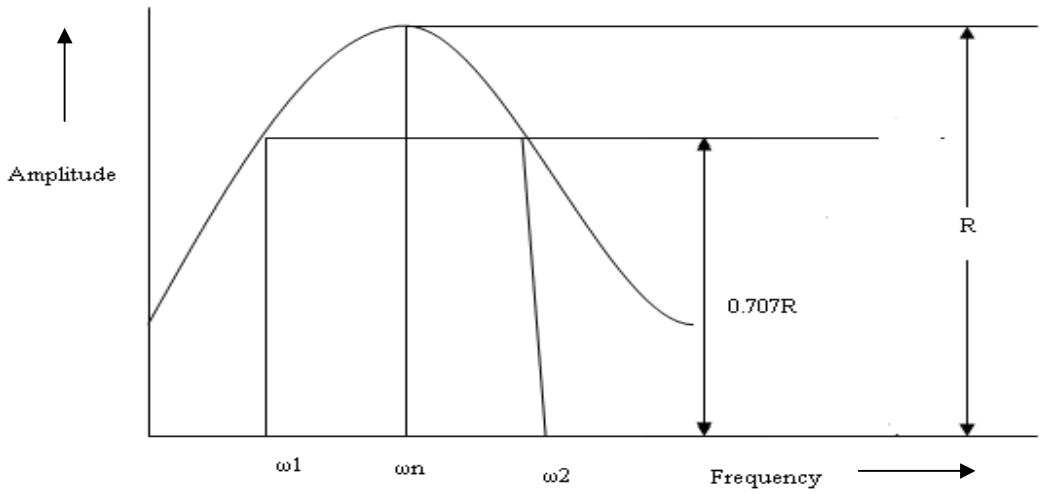

Fig 7.11 Determination of equivalent viscous damping from the frequency response

These values are based on dashpot model developed taking into consider the viscosity of blood and synovial fluid etc. The range of values corresponds to the variation in the length of the segments and diameter in the dash pot model (Y% of L, X% of D)

The damping values at fundamental mode of each segment have been evaluated from frequency response plot (Fig.7.1-7.10) given in Table 7.4

Table 7.4 Damping values at fundamental mode of each segment

Segments of the body	**Theoretical damping value range (Table 5.3)**	**Clearance(e=X%D) and Length of the piston(l=Y%L) (Table 5.3)**	**Damping values at fundamental mode(ξ) cal. by eq. 7.1**
HEAD	0.0159-0.170	1%D, 1-9%L	0.072
NECK	0.0104-0.0813	1%D, 1-9%L	0.069
U.TORSO	0.010-0.0541	1%D, 1-9%L	0.041
C.TORSO	0.020-0.180	1%D, 1-9%L	0.039
L.TORSO	0.018-0.083	1%D, 1-9%L	0.034
U.ARM	0.015-0.583	3%D, 1-9%L	0.018
L.ARM	0.083-1.2	3%D, 1-9%L	0.017
U.LEG	0.011-1.3	3%D, 1-9%L	0.0126
L.LEG	0.0054-0.192	3%D, 1-9%L	0.00603
FEET	0.004-0.175	3%D, 1-9%L	0.0045

Where, e = clearance between the piston and cylinder

l = length of piston

D = Diameter of the segment (Value of D taken from Table 5.1)

L = length of the segment (Value of L taken from Table 5.1)

It is observed that the damping value range as obtained from Eg. 7.1, and shown above, for various segments of body at fundamental mode, lie in between the range of analytical damping values as evaluated in Table 5.3. Also it can be seen from the Table 7.4, the X% of D and Y% of L for modeling dashpots are different for upper segments of the body (head, neck, u.torso, c.torso, l.torso) but lower segments of body (u.arm, l.arm, u.leg,

l.leg, feet). It is therefore dashpot of the upper segment of the body and lower segment of the body is to be modeled separately.

From the above it can be easily concluded that the damping in human body segments as modeled by a viscous dashpot in this work is corroborated with the damping values as obtained from the frequency plots for the fundamental mode for the various body segments. Thus, the frequency response plots and the dashpot modeling both appear to be right approach for studying those aspects of the human body vibration studies.

7.6 Comfort Investigation

To determine comfort as a function of excitation frequency and acceleration amplitude (rms), the British Standard 6841 is shown in Fig.2.3. The values of acceleration (0.5-3.0 m/s^2, 3.0-7.0 m/s^2, 7.0-10.0 m/s^2, 10.0-15.0 m/s^2) corresponding to the frequency (0-10Hz, 10-20Hz, 20-30Hz, 30-40Hz) are shown in graph (Fig. 2.3). It is observed that the excitation frequency range with in which the response of a whole body vibration lies in range of comfort or discomfort depends on acceleration values & duration of exposure. The lines drawn give the threshold values for comfort zone ie. if rms acceleration values for a given duration of exposure and frequency is less than the threshold acceleration then the whole body vibration will be in comfort zone. This excitation frequency range also depends on the acting force.

7.6.1 Calculating r.m.s. acceleration amplitude

The r.m.s. acceleration amplitude value for whole body has been evaluated by the equation, given below

$$acc_{rms} = \sqrt{\frac{1}{n}\sum_{i=1}^{n} X_i^2} = \sqrt{\frac{X_1^2 + X_2^2 + \ldots\ldots + X_n^2}{n}} \qquad (7.2)$$

Where

n= Total no. of body segments

X_1, X_2, X_3, X_4 /X_5, X_6 /X_7, X_8, X_9, X_{10} /X_{11} X_{12} /X_{13}, X_{14}/X_{15} =Acceleration of body segments (head, neck, UT, UA, LA, CT, LT, UL, LL, foot)

Whole body acceleration (m/s^{2}rms) at excitation frequency 2Hz have been calculated by the Eg.7.2 (when force applied at foot), procedure given below

X_1	X_2	X_3	$X_4 = X_5$	$X_6 = X_7$	X_8	X_9	$X_{10} = X_{11}$
0.1913	0.1787	0.1796	0.1922	0.1984	0.1583	0.1419	0.1784

$X_{12} = X_{13}$ $X_{14} = X_{15}$ (all values in mm/s^2)

0.1099 0.0844

Squaring & adding all body segments acceleration values and taking square root of the average,

$$acc_{rms} = \sqrt{\frac{X_1^2 + X_2^2 + X_3^2 + X_4^2 + X_6^2 + X_8^2 + X_9^2 + X_{10}^2 + X_{12}^2 + X_{14}^2}{10}}$$

$$acc_{rms} = \sqrt{\frac{3.6591 + 3.1943 + 3.2259 + 3.692 + 3.9381 + 2.5044 + 2.0143 + 3.1809 + 1.2078 + .7123}{10}}$$

Whole body acc. (m/s^2rms) at 2Hz= 0.1653 mm/s^2 (when force is applied at foot)

Similarly at different excitation frequency (when force is applied at foot)

0Hz=0.006mm/s^2, 4Hz=0.1779 mm/s^2, 6Hz= 0.2179 mm/s^2, 8Hz=0.2742 mm/s^2, 10Hz=0.363 mm/s^2, 12Hz=0.3297 mm/s^2, 14Hz=0.3325 mm/s^2, 16Hz=0.2114 mm/s^2, 18Hz=0.184 mm/s^2, 20Hz= 0.1851 mm/s^2, 22Hz=0.1856 mm/s^2, 24Hz=0.181 mm/s^2, 26Hz=0.173 mm/s^2, 28Hz=0.1734 mm/s^2, 30Hz=0.1738 mm/s^2, 32Hz=0.168 mm/s^2, 34Hz=0.1683 mm/s^2, 36Hz=0.1703 mm/s^2, 38Hz=0.1657 mm/s^2, 40Hz= 0.1674 mm/s^2.

Similarly at different excitation frequency (when force is applied at hand)

0Hz=0.181mm/s^2, 2Hz=4.451 mm/s^2, 4Hz=3.589 mm/s^2, 6Hz= 4.663 mm/s^2, 8Hz=6.644 mm/s^2, 10Hz=7.052 mm/s^2, 12Hz=4.738 mm/s^2, 14Hz=3.791 mm/s^2, 16Hz=2.641 mm/s^2, 18Hz=3.406 mm/s^2, 20Hz= 7.0 mm/s^2, 22Hz=2.131 mm/s^2, 24Hz=1.299 mm/s^2, 26Hz=1.248 mm/s^2, 28Hz=1.470 mm/s^2, 30Hz=1.262 mm/s^2, 32Hz=1.052 mm/s^2, 34Hz=1.054 mm/s^2, 36Hz=1.030 mm/s^2, 38Hz=1.0 mm/s^2, 40Hz= 0.898 mm/s^2

Table 7.5 Whole body acceleration when force applied at foot and at hand

F(Hz)	100 N Force applied at foot and at hand	
	Whole body acceleration(mm/s^2 r.m.s*100)at foot	**Whole body acceleration(mm/s^2 r.m.s*10)at hand**
0	0.6	1.81
2	16.50	44.51
4	17.79	35.89
6	21.79	46.63
8	27.42	66.44
10	36.30	70.52
12	32.97	47.38
14	33.25	37.91
16	21.14	26.41
18	18.40	34.06
20	18.51	70.00
22	18.56	21.31
24	18.10	12.99
26	17.30	12.48
28	17.34	14.70
30	17.38	12.62
32	16.80	10.52
34	16.83	10.54
36	17.03	10.30
38	16.57	10.04
40	16.74	8.98

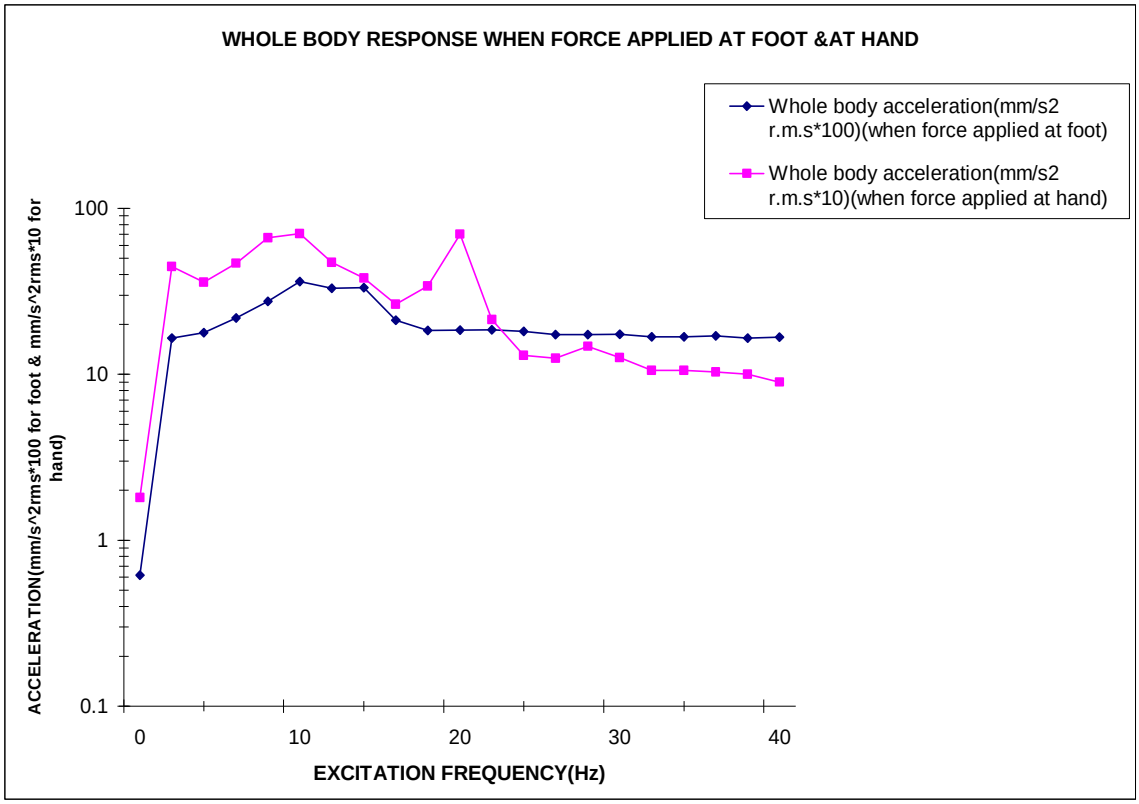

Fig 7.12. ACCELERATION OF WHOLE BODY FOR FORCE=100N ON M14/M15 (FOOT) AND M6/M7 (HAND)

From the Table 7.5 and Fig 7.12, comfort or discomfort ranges for the whole body are $16.5*10^{-2}$-$36.3*10^{-2}$ mm/s^2 rms (when 100N force is applied at foot) and $8.98*10^{-1}$-$70.5*10^{-1}$ mm/s^2 rms (when 100N force is applied at hand). It is seen that whole body acceleration is nearly constant after 18Hz (when force is applied at foot) and after 22Hz (when force is applied at hand).

The comfort of human body depends on the value of acceleration (mm/s^2 rms) and this is also function of duration of exposure and excitation frequency.

One can study the comfort/discomfort to which a human being is subjected to the whole body vibration, with the help of a graph as given above and the duration of exposure in conjunction with the British standard 6841 (Fig.2.3).

Chapter-8

CONCLUSIONS AND SCOPE FOR FUTURE WORK

8.1 CONCLUSION

Experiment and analytical studies conducted on the human body suggest that whole body vibration can cause spinal injury which results in low back pain. Most of the research reported in the literature on human body vibration has used sinusoidal motion to approximate the stimulus to the body. The human body is an immensely complex active multi body dynamic system, the properties of which vary with time. However the most important objective is to analyze and find procedures and method to minimize the effects of vibration on the human body based on such a model.

The object of the present work was to develop a generalized approach towards human body vibratory modeling including damping considerations. The background available to this work was the approach of Nigam and Malik .who proposed that an undamped spring mass vibratory model of human body can be framed through the anthropomorphic model and using the anthropometric data and some elastic properties of the bones and tissue.. The problem was then to introduce damping in the basic spring mass model. This has been done first by calculating the damping coefficients of the various segments of the anthropometric model and using the anthropomorphic data, clearance values and viscosity of blood. The damping ratios of the segments are obtained through their mass, stiffness and damping coefficients and then comparing with experimental values available in literature.

The methodology in the development of complete vibratory model of human body may be summarized as under

1. Identification of segments and their geometrical shapes through anthropomorphic model.
2. One of the important outcome of this thesis has been to obtain the clearance and length of the piston, representing a viscous model, of each segment by using anthropometric data. Certain range of clearance values and length of the piston, have been identified, and are given in Table 5.4.
3. Calculation of damping coefficients using clearance, length and viscosity of blood.

4. Calculation of damping ratio using mass, stiffness and damping coefficients and then comparing with experimental values available in literature.
5. Frequency response curve for constant force excitation at foot and hands have been plotted for all segments of the vibratory model and comparing the resonance frequency with the experimental data of 50^{th} percentile male available in literature.
6. The combination of excitation frequency and location of mass segments vis-à-vis to the point of excitation plays an important role.

8.2 SCOPE FOR FUTURE WORK:

The damping coefficients of the vibratory model in this work have been developed by assigning some appropriate clearance values to individual segments, in order to understand more accurately the behavior of human body, each mass may be further segmented into small number of segments. However the theoretical response of the model shows deviation from the actual response and hence further refinements in the determination of damping coefficients are certainly needed.

The certain low order peaks which are visible in damped response plots but are not observed in the Eigenvalues as determined by Jacobi method for a above model, this needs further investigation.

In order to understand the behavior of human body system in sitting posture. From the sitting posture the vibration behavior human body during the use of earth moving vehicles and other moving machine and machine tool can be evaluated.

REFERENCES

1. **Goldman, D.E., and Von-Gierke, H.E**., "*Effects of shock and vibration on man"*. Chap. 44 of Shock and Vibration Hand Book, Vol 3, 1961.
2. **Pradko, Lee F., and Greene J.D**. "*Human vibration response theory*". Journal of Biomechanics, pp. 205-222 (1967).
3. **Pradko, Richard lee, Victor kaluja**, "*Theory of Human Vibration Response*" Journal of ASME, Biomechanics Monograph, pp.210-222 (1967).
4. **Huston R..L. and Passerello C.E.** "*On the Dynamics of Human Body Model*". Journal of Biomechanics, Vol.4, pp.369-378 (1970)
5. **Bartz A. J., Gianotti.C.R**, "*Computer Program to Generate Dimensional and Inertial Properties of the Human Body*", Journal of Engineering for Industry, Vol.97, pp.49-57, (1975)
6. **Garg P.Devendra and Ross A.Michael** " *Vertical Mode Human Body Vibration Transmissibility*", Journal of IEEE transaction on systems, man and cybernetics Vol. SMC-6, No.2, pp.102-112 (1976)
7. **Muksian Robert and Nash Charles D**. "*On Frequency –Dependent Damping Coefficients in Lumped- Parameter Models of Human Beings*", Journal of Biomechanics, Vol.9, pp.339-342 (1976).
8. **Hatze H**." *A Complete set of control Equations for the Human Musculo-skeletal System"*, Journal of biomechanics Vol.10, pp. 799-805 (1977).
9. **Hatze H**." *A Mathematical model for the Computational Determination of Parameter Values of Anthropometric Segments*", Journal of Biomechanics Vol.13, pp. 833-843 (1980).
10. **Hatze H**." *A Comprehensive Model for Human Motion Simulation and its Application to the Take-off phase of Long jump*", Journal of biomechanics Vol.14, pp. 135-142 (1981).
11. **Engin A.E**. *"On the Damping Properties of the Shoulder Complex*", Transaction of ASME, Journal of Biomechanics, Vol. 106 No.4, pp.360-363 (1984).
12. **Patil K.Mothiram**, "*Minimization of Human Body Responses to Low Frequency Vibration: Application to Tractors and Trucks*". International Journal of Industrial Ergonomics vol. 6, pp421-422, (1985).

13. **Nigam S.P. and Malik M** "*A Study on a Vibratory Model of a Human Body*", Transaction of ASME, Journal of Biomechanics, Vol. 109, pp. 148-153 (1987).
14. **Singh N. et al**, "*Analytical Determination of Frequency Response Characteristics of a Human Body*", IE (I) journal –(1987)*
15. **Gupta T.C**., "*Development of Human Body Vibration Model through Anthropomorphic Segments*". M.E. Dissertation, MIED, UOR, Roorkee, (1988)
16. **James, M.L., and Smith,G.M**., "*Vibration of Mechanical and Structural System*", Book.(1989).
17. **Griffin J.M.** "*Measurement and Evaluation of the Whole Body Vibration at Work*" International Journal of Industrial Ergonomics (1990)*.
18. **Nigam S.P., Singh N., and Grover G.K**., "*Study of vibratory response characteristics of human body through analytical modeling*", Journal of Engineering for Industry (I), Vol. 72, pp. 12-17 (1991)..
19. **Nigam S.P. and Malik M**. "*Mechanical Analogue of a Human Body*" , 4th ISME Conference journal IE. (1991).
20. **Kapur, J.N**.,"*Mathematical models in Biology & Medicine*", East-West Press Pvt. Ltd. (1992).
21. **Amirouche, F. M.L., et. al**., *"Optimization of the Contact Damping and Stiffness Coefficients to Minimize human Body Viberation*", Journal of Bio-mechanical Engg. Vol. 46, pp. 413-420 (1994)
22. **Qassem, w**., "*Model Predication of Vibration Effects on Human Subject Seated on Various Cushions*". Journal of Medical Engg. And Physics. Vol.18, No.5, pp.350-358 (1996).
23. **Chen S.Y. et al**. "*Estimation of Mass, Stiffness and Damping Matrices from Frequency Response Functions*", Transaction of ASME Journal of Vibration. Vol. 118, pp. 78–82. (1996).
24. **J.Gold Berg**, "High Frequency dynamics of human head-neck system", Baylor college of medicine, **,** Journal Session, Vol. 390 (1997).
25. **Wei W., and Griffin J**., "*The Predication of Seat Transmissibility from Measures of Seat Impedance*", Journal of Sound and Vibration, Vol.214 (1), pp.121-137. (1998).

26. **Griffin J.M**. "*Modeling the Dynamic Mechanisms Associated with the Principal Response of the Seated Human Body"* Clinical biomechanics16 Supplement no 1, pp. 31-44. (2001).
27. **Grover G.K.** "*Mechanical Vibration*" Seventh Edition ,2003 Nem Chand & Bros. Roorkee, INDIA.
28. **Rosen J. and Mircea A**.*" Modeling the Human Body/Seat System in a Vibration Environment*" Journal of Biomechanical Engineering,Vol.125 pp.223-231 (2003)
29. **Mansfield Nel J. and Meada Setuso** "*Comparison of the apparent mass and cross-axis apparent masses of seated humans exposed to single and dual-axis whole body vibration.*" Journal of Sound and Vibration, Vol.298 (1), pp.841-853, (2006).
30. **Ayres Frank, "***Theory and Problem of Matrices"* Schaum's outline, Sixth Edition, 2006, Tata McGraw Hill, New Delhi
31. **Rutrel Sebastain et al** "*Model description – A better way of characterizing human vibration behavior*" Journal of Sound and Vibration, Vol.298 (3), pp.810-823 (2006).
32. **H. Nelisse, S. Patra, S. Rakheja, J. Boutin**, " *Assessments of two dynamic Manikins for laboratory testing of seats under whole-body vibration*" International Journal of Industrial Ergonomics, Article in press (2007)